

STUDY REPORT

SR 289

(2013)

Remediating Condensation Problems in Large-Cavity, Steel-Framed Institutional Roofs

MJ Cunningham and L Quaglia



The work reported here was jointly funded by BRANZ from the Building Research Levy.

© BRANZ 2013
ISSN: 1179-6197

Preface

This is the final report prepared during research into condensation problems in large-cavity, steel-framed institutional roofs and ways to mitigate them.

Acknowledgments

This work was funded by the Building Research Levy.

Note

This report is mainly intended for researchers interested in roof moisture problems.

Remediating Condensation Problems in Large-Cavity, Steel-Framed Institutional Roofs

BRANZ Study Report SR 289

MJ Cunningham and L Quaglia

Reference

Cunningham M.J. and Quaglia L., 2013, Remediating condensation problems in large-cavity, steel-framed institutional roofs, BRANZ Study Report SR 289, BRANZ Ltd, Judgeford, New Zealand.

Abstract

There has been an increasing number of reports of excessive condensation within the roofs of institutional buildings in New Zealand over the last few years. These roofs have a common similar design entailing large roof cavities, profiled metal roofs with underlay, metal framing, batt insulation on the ceiling and acoustic tile suspended ceilings. Some condensation was appearing under the metal roofs, but these roofs are designed to tolerate this occurrence and so was not the problem condensation mechanism. Rather, unexpectedly, condensation controlled by a continuous underlay was collected on the metal structural elements particular the roofs' metal purlins. An understanding of this condensation mechanism and how to avoid it is the subject of this report.

Through an experimental and modelling approach we show that the traditional practice of using a thermal break between steel elements and the roof is not always sufficient to avoid condensation in these roofs, and that full cover board insulation systems above the main cavity are often needed. We show that condensation did not appear in the pattern predicted: condensing under the metal roof expected early in the morning, particularly on frosty nights, was inhibited by the hygroscopic properties of the underlay; and in the roofs without board insulation, after significant rain effects, condensation appeared after sunrise of the next day. Critical to the experimental success of the study was the accurate and non-linear calibration of relative humidity (RH) sensors in the difficult range of 95% to 100% RH.

We also show that, for the roofs investigated, their moisture contents and condensation episodes are determined by ventilation from indoors and outdoors which dominates over both diffusion and hygroscopic storage effects, and that consequently the key parameter in understanding the hygrothermal performance of these roofs is the ratio of outdoor to indoor ventilation values.

We finish the report by using a modelling approach to derive design charts allowing the user to choose the insulation thickness and roof ventilation levels or modify the indoor climate to limit the amount of condensation that may accumulate in these structures.

1. NOMENCLATURE

Roman Letters

<i>A</i>	area	m^2
<i>Ce</i>	dimensionless number	
<i>Ci</i>	dimensionless number	
<i>F</i>	air change rate	s^{-1}
<i>P</i>	air pressure	Pa
<i>Q</i>	air flow	$m^3 h^{-1}$
<i>r</i>	vapour resistance	$N s kg^{-1}$
<i>R</i>	universal gas constant	$8310 J K^{-1} kmole^{-1}$
<i>t</i>	time	s
<i>T</i>	Kelvin temperature	K
<i>V</i>	volume	m^3
<i>W</i>	molecular weight of water	18 kg/kmole

Greek letters

α ventilation fraction

Subscripts

a transport by air
c cavity or ceiling
d transport by diffusion
eff effective
h hygroscopic material
i indoors
o outdoors
v vapour

Contents	Page
1. NOMENCLATURE	IV
2. INTRODUCTION.....	8
3. METHODS.....	10
3.1 Shipping container experimental rig	10
4. ROOF SPECIMENS.....	15
4.1 Common elements.....	15
4.2 Timber thermal breaks specimen.....	15
4.3 Phenolic insulation sandwich specimen.....	15
4.4 EPS insulation board specimen	16
4.5 EPS metal panel specimen.....	16
4.6 Some fire safety considerations	17
5. INSTRUMENTATION.....	18
5.1 Control of the indoor environment.....	19
5.2 Measurement of air flow characteristics	20
6. RESULTS.....	22
6.1 Phenolic roof	22
6.2 Timber roof	22
6.3 EPS roof	22
6.4 Metal panel roof	22
6.5 Condensation events	26
6.6 No night condensation events.....	29
6.7 Measurement of air flow characteristics	31
6.8 Estimation of ventilation rates	34
6.9 The relative importance of ventilation, diffusion and hygroscopic moisture fluxes 36	
7. MODELLING.....	39
8. DESIGN.....	41
8.1 Roof type	41
8.2 Loadings	41
8.3 The amount of insulation	41
8.4 Ventilation levels.....	41
8.5 Achieving the required ventilation levels	42
9. FURTHER WORK.....	45
10. DESIGN CONCLUSIONS	45
11. GENERAL CONCLUSIONS.....	46
12. REFERENCES.....	47

13. APPENDIX.....	48
13.1 Ventilation requirements in some overseas building codes	48

Figures	Page
Figure 1: Diagram shows how a container represents a section of a commercial building roof.....	10
Figure 2: Pictures of the 40ft container with the roof removed.	11
Figure 3: Drawing of the roof frame of the commercial roof specimen. The roof specimen is intended to represent a full-scale section of a commercial roof.....	12
Figure 4 Vertical section of the roof specimen. From top to bottom, we have the profiled metal cladding, underlay, safety wire netting, section of three universal beams, a pair of purlins with the corresponding cleats, an air gap, fiberglass insulation and perlite acoustic tiles.	13
Figure 5: Picture of the Roof Test Facility. We can see the container supporting the commercial roof specimen. Notice the plywood sheets closing off the side of the specimen. Also visible is the scaffolding used to work around the roof.	13
Figure 6: Roof design with a simple thermal break: a timber purlin over the metal purlin.	15
Figure 7: Roof design with phenolic insulation panels.	16
Figure 8: Roof design with a full thermal break: timber purlins and EPS panels in between.	16
Figure 9: Roof design with full thermal breaks: EPS panels protected by two thin metal sheets.	17
Figure 10: Position of the RH/T sensor pair.	18
Figure 11: Idealised school room climate used in this study. The “very wet” climate was used in the container. All climate types were used in the modelling.	19
Figure 12: Schematic of a pressurisation test of the roof space where the air flow through the ceiling has been dynamically “cancelled out” by using a second fan to reduce the pressure difference ΔP_2 to zero.	21
Figure 13: Cross sections through the roof at selected times (horizontal axis categorical, i.e. not scaled).....	23
Figure 14: Psychrometric conditions for representative periods for the purlin air of the phenolic roof.....	24
Figure 15: Psychrometric conditions for representative periods for the air adjacent to the purlin of the timber roof.	24
Figure 16: Psychrometric conditions for representative periods for air adjacent to the purlin of the EPS roof.....	25
Figure 17: Psychrometric conditions for representative periods for air adjacent to the purlin of the panel roof.	25
Figure 18: Histogram of relative humidities of the air adjacent to the metal purlins (includes rain events).	26
Figure 19: Histogram of high relative humidities of the air adjacent to the metal purlins for roofs with timber and EPS roofs (includes rain events).....	26
Figure 20: A condensation episode happens on the purlin flange the morning after a period of rain.	27
Figure 21: Histogram of relative humidities of the air in the small cavity above the underlay and below the cladding (includes rain events).	28
Figure 22: Histogram of high relative humidities of the air in the small cavity above the underlay and below the cladding, for timber and EPS roofs (includes rain events).....	28
Figure 23: Above underlay relative humidity when small cavity above underlay radiatively cooled (phenolic specimen).	29
Figure 24: Above underlay temperatures when small cavity above underlay radiatively cooled (phenolic specimen).	30
Figure 25: Above underlay vapour pressures when small cavity above underlay radiatively cooled (phenolic specimen).	30

Figure 26: Schematic of a pressurisation test of the container space.	31
Figure 27: Schematic of a pressurisation test of the container space after lining its walls with an airtight layer.	32
Figure 28: Schematic of the pressurisation test of the roof space.	33
Figure 29: Schematic of the pressurisation of roof space with air flow through the ceiling cancelled out by means of a second fan.	33
Figure 30: Example of pressure differences between container space and outdoors during a calm and cloudless night.	35
Figure 31: Example of pressure differences between roof space and outdoors during a calm and cloudless night.	35
Figure 32: Very simplified equivalent resistance network schematising the air flow resistances between container space and outdoor, between roof space and outdoor, and across the ceiling.	36
Figure 33: Temperatures in small cavity above underlay for the timber specimen.	39
Figure 34: Experimental and modelled temperatures in the air adjacent to the upper flange of the metal purlin for the EPS structure.	39
Figure 35: Fitting the relative humidity for the EPS specimen by putting ventilation fraction to 0.79.	40
Figure 36: Design graph for a 90 mm thermal break (timber) and no board insulation. There is very little difference in performance between a timber and EPS thermal break.	42
Figure 37: Design graphs by loading for specimens with rigid insulation systems above the main cavity.	43
Figure 38: Design graphs by the R-value of the rigid insulation systems above the main cavity.	44

Tables

Page

Table 1: Prevalence of condensation events.	29
Table 2: Air flow characteristics of various (distributed) openings in the roof specimen and in the container	34
Table 3: $C_{e_{ceiling}}$, the ratio of ventilative to diffusive fluxes in the main cavity of all specimens. $C_{e_{outdoors}}$ is infinite.	37
Table 4: $C_{e_{indoors}}$, the ratio of ventilative to diffusive fluxes in the cavity below the cladding (no cavity for the metal panel specimen). $C_{e_{outdoors}}$ is infinite.	37
Table 5: C_i , the ratio of ventilative to hygroscopic fluxes in the main cavity of each specimen.	38
Table 6: C_i , the ratio of ventilative to hygroscopic fluxes in the cavity below the cladding of each specimen (cavity of all specimens the same size, no cavity for the metal panel specimen).	38
Table 7: Indoor climate parameters.	41
Table 8: Ventilation requirements (in units of 1000 mm ² /m roof width or equivalently height in mm of a continuous vent opening) for roofs under BS 5250:2002, Amendment 1 [15].	49

2. INTRODUCTION

There has been an increasing number of reports of excessive condensation within the roofs of institutional buildings in New Zealand over the last few years. Investigation of several of these roofs found that all were of similar design. They have large roof cavities, profiled metal roofs with underlay, metal framing, and batt insulation on the ceiling and acoustic tile suspended ceilings Figure 3 and Figure 4 show the structural details of these roofs.

It was clear that high air humidity from the classroom was passing into the roof space and condensing on some parts of the metal framing when it was sufficiently cold. To prevent condensation, sheathing of a sandwich construction of phenolic insulation between plywood was retrofitted on top of the main rafters and purlins to raise the temperature of the framing and the roof cavity air.

The fix is difficult to construct and expensive, so cheaper retrofit and new designs have been requested. This work describes an experimental and modelling study using four different alternative roof designs so as to identify a design that is cheaper than the phenolic sandwich option, but still avoids condensation while meeting structural, fire and acoustic requirements.

It was taken as a given that the suspended ceiling and profiled metal roof would remain unchanged in any new design, leaving the internal structure of the roof and ventilation levels as the chief variable elements. The current roofs are variants of that shown in Figure 4, where the roof is supported by steel rafters and purlins, with an addition of a thermal break. Of note was that condensation was predominantly forming on the metal purlins and slightly under the profiled metal roof above the underlay but not in the underlay. We show here that the lack of significant condensation under the profiled metal roof is due to the hygroscopic properties of the underlay. On the other hand it is not immediately obvious that condensation should form on the metal elements.

Although designers should always specify a thermal break behind metal wall framing they are less aware that a thermal break is necessary and much less aware it may not be enough in certain roof situations. Particularly if large amounts of moisture can find its way into a roof cavity then condensation may still occur on thermally broken elements. This can happen if the working space below has high relative humidities, if the ceiling is very vapour or air permeable, or if there is inadequate ventilation from outdoors into the roof space. Furthermore, if the framing through which excessive heat is flowing is not connected to the ceiling then its temperature is determined partly by the temperature of the cavity air, not partly by the indoor temperature. Thus the temperature of this framing is even lower than what it would have been if it was connected to the ceiling, over any period that the cavity air temperature is below the indoor temperature, aggravating any condensation issues.

The thermal break literature has little to say about this circumstance. Our understanding of the thermal consequences of simple thermal bridges and how to avoid them is considered to be mature and standard methods are available to calculate their thermal impact [1, 2]. Consequently designers are aware of the need for thermal breaks in metal framing [3]. A paper by Susanti et al [4] examines ventilation in factory roofs but the work addresses cooling rather than thermal bridge-based condensation. A paper in Chinese appears directly relevant [5] but unfortunately an English translation is not available. In its abstract it is stated that for light steel roofs, the outer cladding can be very cold but the vapour pressure of the air behind it can be near to indoor conditions, with a strong risk for condensation. The abstract states design details are presented to address this problem.

Otherwise most of the thermal break literature is on wall, wall-floor junctions, floors, balconies etc, for example work by Gorgolewski [6], Zalewski, L., et al [7] with fewer publications for roofs, especially pitched roofs. British Standard 5250 [8] contains extensive advice on avoiding condensation in pitched roofs but is not intended to address the presence of cold metal framing.

This work examines conditions conducive to condensation in a typical New Zealand construction practice, institutional roof, such as schools etc, with steel structural elements, a suspended acoustic tile ceiling and metal roof with underlay. It is not primarily concerned with condensation under the roof, but rather with unexpected condensation on the steel members including metal purlins. (In the New Zealand climate, building practice and regulatory environment, condensation under metal roofs is usually acceptable, with the roof underlay designed to catch condensation drip and prevent it penetrating deeper into the structure).

With an experimental and modelling approach we show that the traditional (and occasional) practice of using a thermal break between steel elements and the roof is not always sufficient to avoid condensation, and that full cover board insulation systems above the main cavity are often needed. We show that condensation did not appear in the pattern predicted: condensing under the metal roof expected early in the morning, particularly on frosty nights, was inhibited by the hygroscopic properties of the underlay; and in the roofs without board insulation, after significant rain events, condensation appeared after sunrise of the next day. We also show that, for the roofs investigated, moisture contents and condensation episodes are determined by ventilation from indoors and outdoors which dominates over both diffusion and hygroscopic storage effects, and that consequently the key parameter in understanding the hygrothermal performance of these roofs is the ratio of outdoor to indoor ventilation values.

We finish the report by using a modelling approach to derive design charts allowing the user to choose the insulation thickness and the roof ventilation levels or modify the indoor climate to limit the amount of condensation that may accumulate in these structures. There are many roof models available. Burch, Tsongas [9] and Walton examine the effect of envelope details including ventilation on the moisture content of plywood sheathing in manufactured homes using the program MOIST. Roof cavity ventilation is calculated with a flow resistance model. Sanders [10] developed a model called Roofcond which was designed for sensitivity analysis and is based on very broad brush "rules of thumb". Nelson and Ananian [11] using WUFI [12] modelling favour venting over non-venting in roofs with asphalt shingles as construction moisture or water from leaks dries only slowly in non-venting roofs.

In this work we use WUFI and exploit the fact that our roof specimens are ventilation-dominant. This leads to simplification in the modelling of the effect of ventilation on our roof specimens.

3. METHODS

3.1 Shipping container experimental rig

The experimental part of the research is based around a purpose-built, full-scale section of a commercial roof, shown schematically in Figure 1.

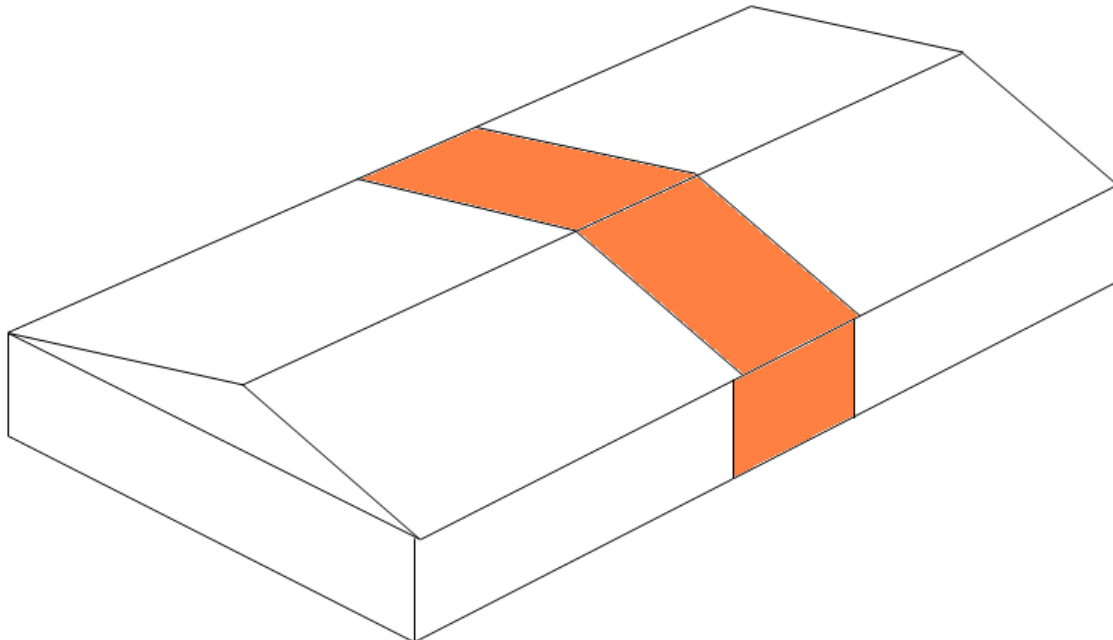


Figure 1: Diagram shows how a container represents a section of a commercial building roof.

As Figure 1 illustrates, we experimentally recreate a section cut out of the whole roof and mount it on a 40 ft shipping container, see Figure 2 to Figure 5.

We chose to use a container instead of building a fixed structure on the BRANZ campus for two reasons: mobility and flexibility. A container allows the Roof Test Facility to be shifted to other parts of the country where the conditions may be more prone to condensation problems than those experienced in Wellington. A container also allows the installation of roof specimens of different kinds. A commercial roof specimen with its metal structure or a residential roof specimen with its timber structure can be relatively easily fitted and attached to the tubular frame of the container.

The roof of the container was removed, just leaving the tubular frame at its perimeter (see Figure 2). The tubular frame provides the support for construction of the roof specimens to be investigated during the project.

While on the BRANZ campus the container rests on a platform made of piles and load bearers. The long axis of the platform and hence the container and its roof is roughly oriented north-south. We chose that alignment because the prevailing winds in the Wellington region are from the northwest and the south. Moreover, the north-south orientation allows for symmetrical exposure of the building and for the slopes of the roof to solar irradiation.



Figure 2: Pictures of the 40ft container with the roof removed.

We insulated the gap between the ground and the underfloor of the container with 200-millimetre-thick polystyrene panels. A polyethylene sheet was also laid on the ground under the insulating panels in order to provide a partial barrier to dampness rising towards the timber floor of the container.

The walls of the container were also insulated using 100-millimetre-thick polystyrene panels. These panels were chosen instead of the more conventional fibreglass or polyester wall insulation because they are rigid and compact, and do not require the presence of wall framing which is naturally absent in a container. We fixed the panels to the timber floor with the help of metallic square brackets and a long piece of timber screwed on the top of the walls.

Figure 3 shows the structure of the roof framing. The roof specimen has two slopes, one oriented due-north and one oriented due-south. The roof frame is made up of three couples of universal beams resting on top of the short walls of the container and joined at the ridge. Twelve couples of C-shaped metal purlins span between the universal beams and are fixed to them by cleats. All parts of the roof frame are screwed together and no elements are welded together so that the specimen can be entirely disassembled and changed to a totally different structure.

A section of the structure of the most simple roof specimen built around the metallic roof frame is shown in Figure 4. From top to bottom, we can see the profiled metal cladding, fire retardant underlay, safety wire mesh, section of the three universal beams, metal purlins fixed to the universal beams, an air gap, fibreglass insulation and the ceiling made of acoustic insulating tiles. The ceiling is of the suspended type, formed by a lightweight metal frame supported by hangers fixed to the purlins, which holds the ceiling tiles in place.

The vertical long sides of the roof are closed off by 20-millimetre-thick marine-grade plywood panels as seen in Figure 5. The main axis of interest for the exchange of heat, air and moisture in the roof specimen is the north-south axis. Considering that the roof specimen is just a section of a full-scale roof which would be much wider in the east-west direction, the exchanges of heat, air and moisture laterally through the sides of the roof specimen are ideally zero.

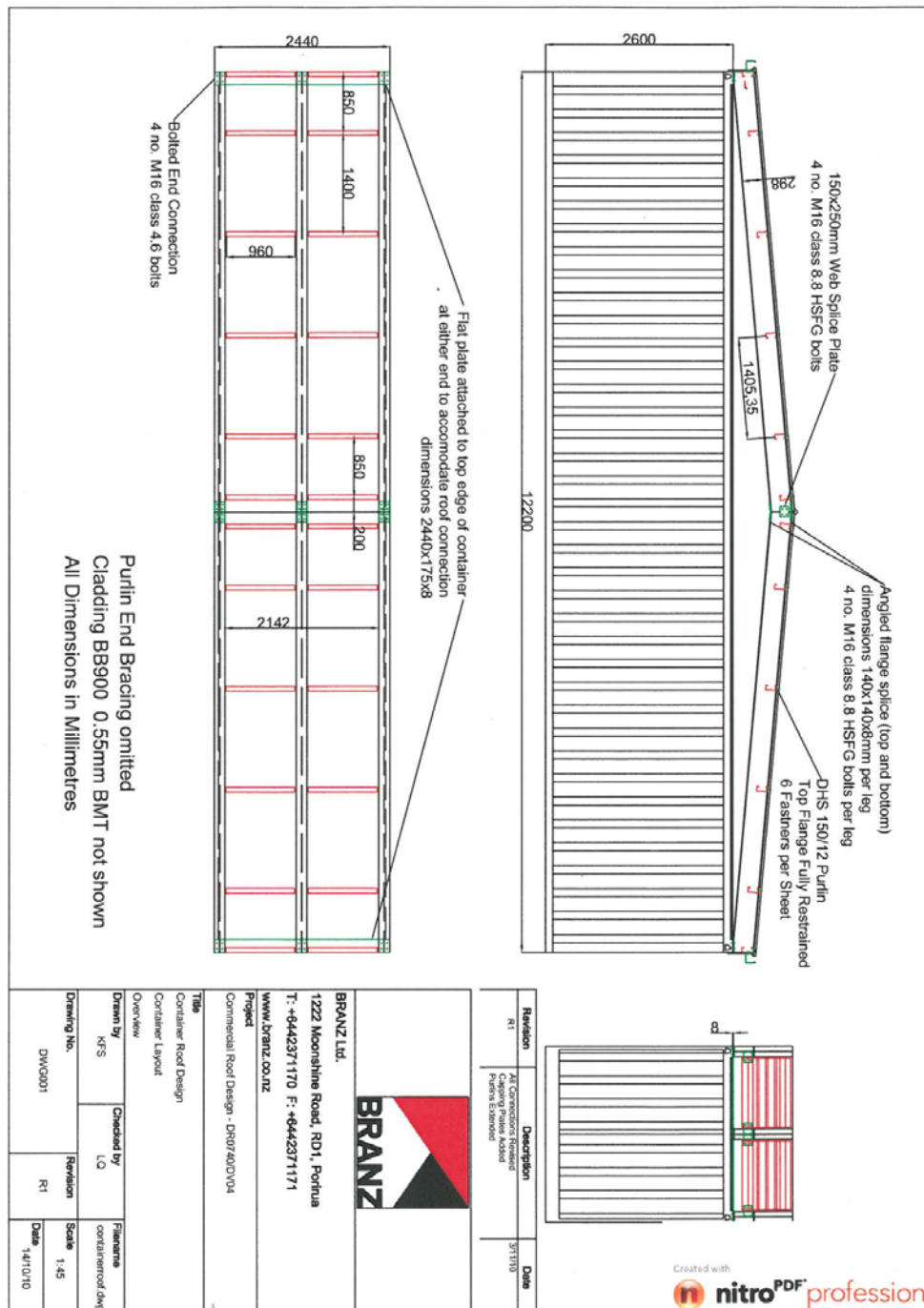


Figure 3: Drawing of the roof frame of the commercial roof specimen. The roof specimen is intended to represent a full-scale section of a commercial roof.

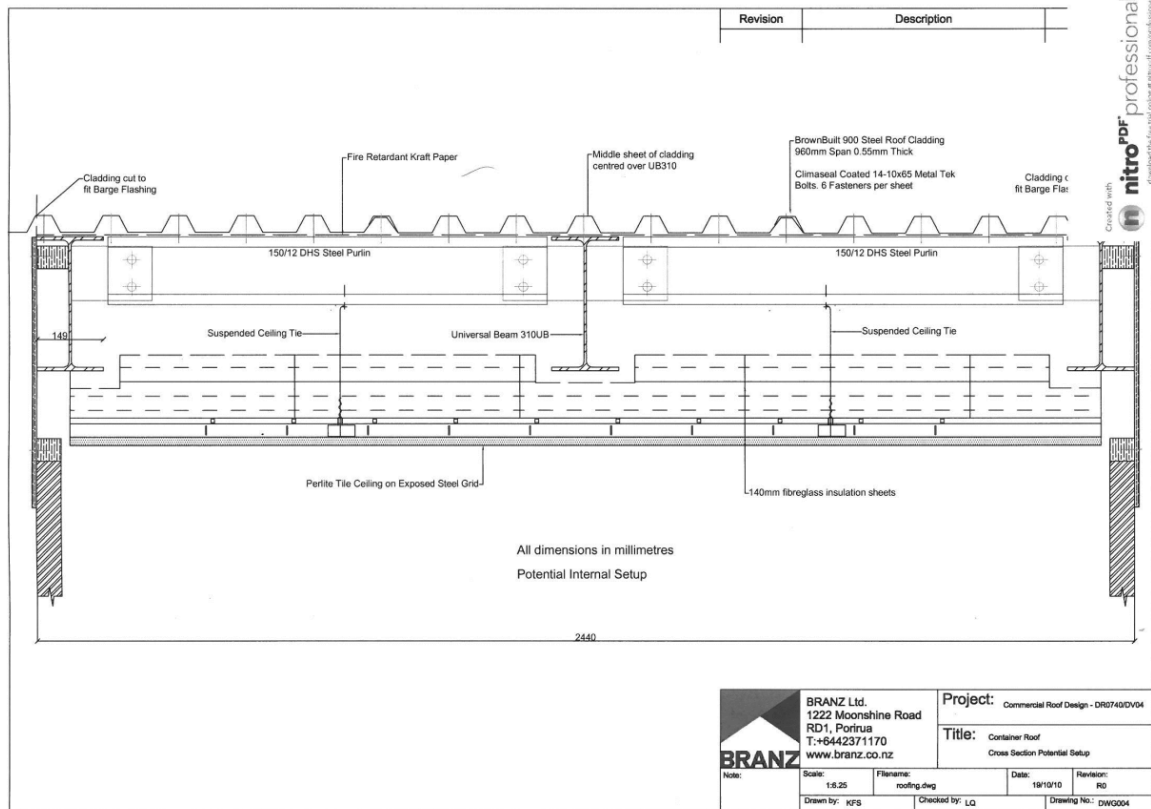


Figure 4 Vertical section of the roof specimen. From top to bottom, we have the profiled metal cladding, underlay, safety wire netting, section of three universal beams, a pair of purlins with the corresponding cleats, an air gap, fiberglass insulation and perlite acoustic tiles.



Figure 5: Picture of the Roof Test Facility. We can see the container supporting the commercial roof specimen. Notice the plywood sheets closing off the side of the specimen. Also visible is the scaffolding used to work around the roof.

In order to minimise lateral moisture transport, a continuous polyethylene sheet was installed behind the plywood sheets to cover the space between the outer side of the universal beams at the edge of the specimen and the top of the long walls of the container. This sheet provides an impervious vapour barrier. To minimise the lateral transport of heat through the sides of the specimen, the space behind the plywood sheets and the polyethylene barrier and between the top of the wall and the underside of the universal beams was insulated with 135-millimetre-thick polystyrene panels. The space between the bottom and top flange of the universal beams was also insulated with polystyrene.

To ensure the weathertightness of the roof specimen, metal flashings were installed at the ridge of the roof and along the junction between roof cladding and plywood side panels.

The container was trucked and shifted down to Dunedin from BRANZ in Wellington and four different roof specimens tested over the period from 4 July 2012 to 8 October 2012, i.e. the second half of a Southern Hemisphere winter. During this time the average outdoor temperature was 8.2°C, with a minimum of -1.4°C and a maximum of 25.2°C. The average outdoor relative humidity was 81%.

4. ROOF SPECIMENS

4.1 Common elements

All roof specimens except the EPS metal panel, see below, have a common roof and building underlay cladding system.

The roof cladding is metal with a trapezoidal profile and is fixed to the metal purlins with screws which traverse whatever thermal break system is installed in between.

The building underlay is of kraft paper with the addition of fire retardant salts and is hygroscopic with 13% equilibrium moisture content at 100% relative humidity. It has a water vapour resistance of 2.5 MN s/g at 75% relative humidity and an area density of 450 g/m².

4.2 Timber thermal breaks specimen

Hereafter called the “timber specimen”, depicted in Figure 6, this roof has a timber purlin on top of the metallic purlin to act as a thermal break. The cladding can radiatively cool well below ambient temperatures on frosty nights but is now thermally separated from the metal purlin by this timber purlin. One drawback of this design is that the air inside the roof cavity can be easily cooled down by the cold cladding because most of the surface of the roof is in direct contact with the air inside the roof cavity (the roof underlay has very little influence because it has a very low thermal resistance).

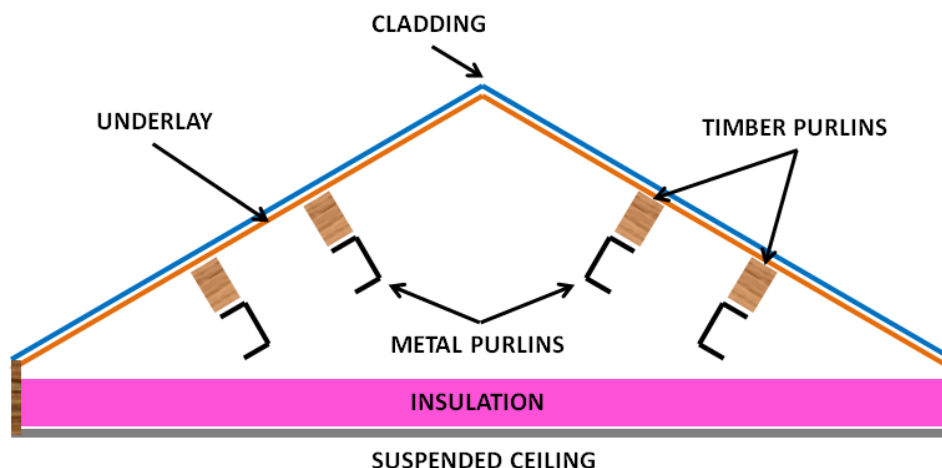


Figure 6: Roof design with a simple thermal break: a timber purlin over the metal purlin.

4.3 Phenolic insulation sandwich specimen

Hereafter called the “phenol specimen”, depicted in Figure 7, this roof represents a more complex way of breaking the thermal bridge which addresses some of the shortcomings of the simple thermal break design. The roof deck is fully insulated from the metallic cladding using insulating panels. Those panels are formed by an insulating material sandwiched within two sheets of plywood. The insulating material was chosen to be a phenolic material for its fire retardant and structural properties. The panels are interlocking using a system of timber shear keys. The timber shear key is a long piece of timber as thick as the phenolic insulation located at the perimeter of the panels and spanning across the edges of neighbouring panels. This provides a system to interlock the panels during construction and stiffen the panels preventing them from sagging.

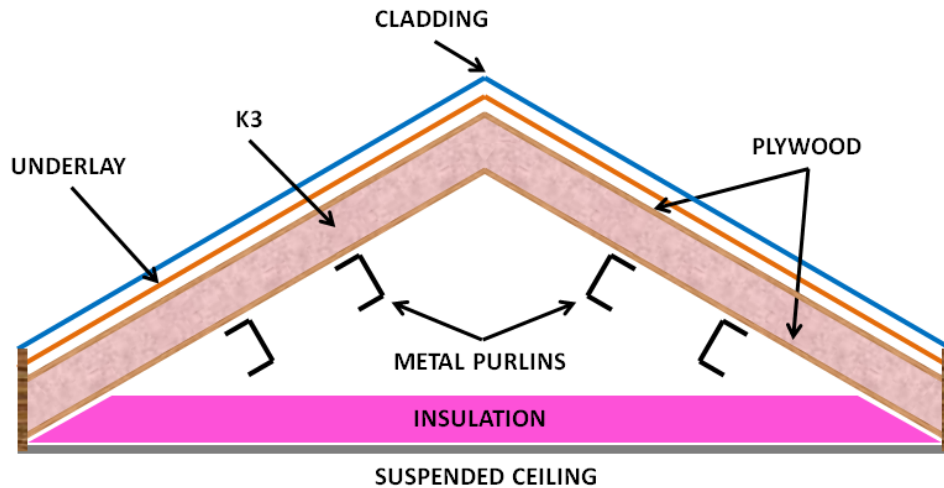


Figure 7: Roof design with phenolic insulation panels.

4.4 EPS insulation board specimen

Hereafter called the “EPS specimen”, as depicted in Figure 8, this is a variation of the previous fully-insulated specimen. The roof deck is insulated by installing timber purlins over the metal purlins and EPS panels in between. Wire mesh spanning over the metal purlins supports the EPS panels and keeps them in place.

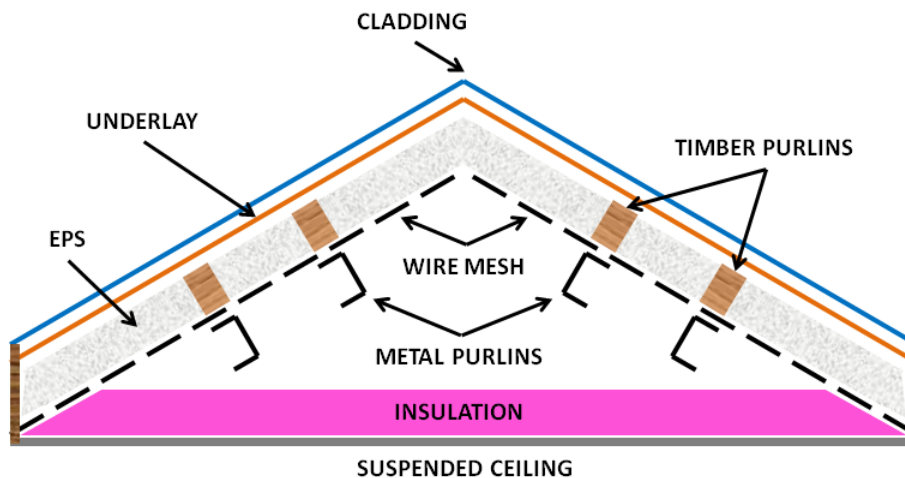


Figure 8: Roof design with a full thermal break: timber purlins and EPS panels in between.

4.5 EPS metal panel specimen

Hereafter called the “metal panel design”, this roof specimen depicted in Figure 9 is another variation of the fully-insulated solution. Interlocking commercial cladding elements formed by EPS panels sandwiched between two thin metal sheets replace the traditional metal cladding used to build commercial roofs.

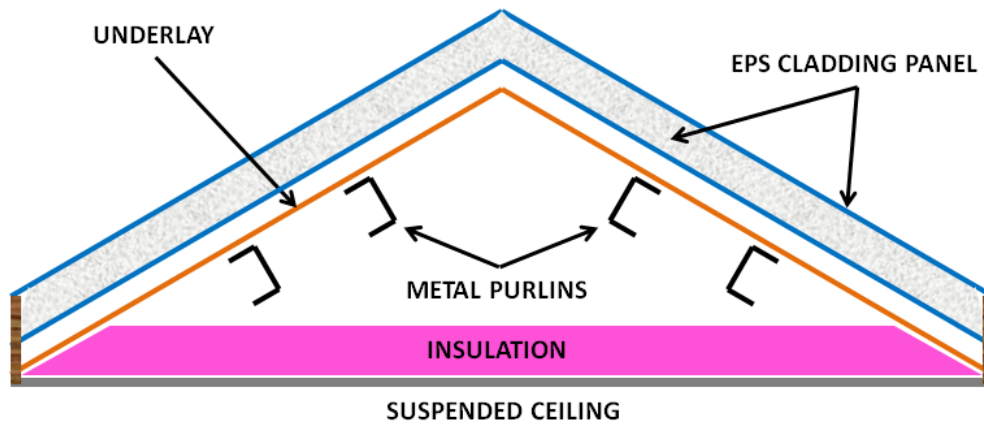


Figure 9: Roof design with full thermal breaks: EPS panels protected by two thin metal sheets.

4.6 Some fire safety considerations

Besides the hygrothermal considerations, any roof assembly needs to conform to the relevant fire safety requirements. It is not possible to judge the fire safety suitability of generic roof assemblies but we will mention some of the requirements that need to be fulfilled.

All roof types include a suspended ceiling system. According to the New Zealand Building Code Acceptable Solution C/AS1 (paragraph 4.2) and Acceptable Solution C/AS2-7 (paragraph 4.17), the surface finish of the ceiling needs to meet the relevant group number.

The roof assemblies which contain EPS boards or phenolic insulation boards need also to meet the flammability requirements for those products as laid out in the Australian Standard 1366.

5. INSTRUMENTATION

The roof is instrumented with a range of monitoring equipment in order to gather information on how the different roof designs are performing. Temperatures are measured using type T thermocouples made of a pair of copper and constantan wires with the reference junction being an isothermal block. A platinum resistance thermistor measures the temperature of the isothermal block to provide the reference temperature for the thermocouple measurements.

Relative humidities are measured using capacitance Honeywell HIH 4000 sensors.

Figure 10 shows a metal purlin as found in all specimens and indicates the position of relative humidity/temperature pairs in this location. Some temperature and relative humidity sensors are directly in contact with the metal surfaces and some are in the air at around 10 mm from the metal surfaces.

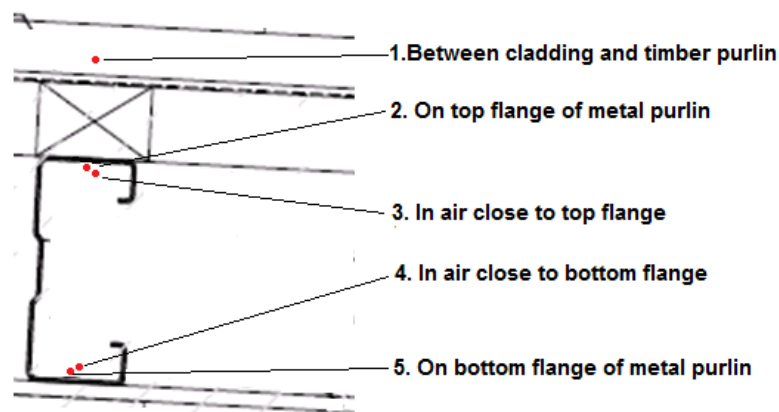


Figure 10: Position of the RH/T sensor pair.

Other quantities monitored are: timber moisture content, ventilation rates, pressure differences and wind speed and direction. The moisture content of the surface of timber elements (i.e. the plywood sheets in the fully-insulated roof design) gives an indication of the trend of condensation and drying over those surfaces. Ventilation can transport important quantities of moisture in and out of the roof space. Pressure differences are the drivers of ventilation and they are important in the study of localised or distributed openings in the roof. The wind speed and direction over the roof is one of the generators of pressure difference, the other being temperature differences (stack effect).

Timber moisture content is measured resistively using thin metallic pins, separated by 10-15 mm, inserted into the timber and driven by 12 V.

Ventilation rates are measured by the constant injection tracer gas technique using CO₂ and/or N₂O. Briefly, the technique introduces the tracer gases at a constant rate into the zones of interest, which are transported to other zones including the outdoors. By measuring the gases' concentration in the monitored zones, mass balance calculations can then be used to establish the air change rate between these zones. The zones of interest in this work are the roof cavity and the indoor space.

We have built an apparatus to automate this measurement which samples air alternatively from the two zones by means of a system of solenoid valves. The air sample is then analysed to detect the concentration of the tracer gases using two GasCard infrared absorption

detectors (Edinburgh Instruments) and the readings were logged with a National Instruments data acquisition unit.

Pressure differences are measured using an MKS Baratron pressure gauge capable of measuring pressure differences in the order of 0.1 Pa. This is the order of magnitude of pressure differences that can be found between zones of a building or the interface between indoor and outdoor. The gauge is self-heated to 40°C in order to minimise the temperature drifts of span and zero.

Very accurate relative humidity measurement of between 95% to 100% is crucial to the success of this study, yet it is well known how difficult this is to achieve. There is not a suitable choice of salt solutions to use as a calibration method in this range and some sensor types do not behave stably in this region. Often relative humidity sensors are calibrated up to 90% or occasionally 95% and a linear calibration curve fitted. This is not adequate for our purposes, so a BRANZ-manufactured two-pressure-relative humidity generator was used to calibrate Honeywell-capacitive sensors percent by percent in the 95% to 100% range and a non-linear calibration curve used. We found that the sensors had a linear response to about 80% and a quadratic response above that. We estimate that the calibrated sensors were accurate to within 1% or 2% humidity above 95% and to within 1% below that.

5.1 Control of the indoor environment

The environment inside the container is actively controlled to provide an idealised school room climate based on actual measurements in New Zealand schools with intermittently-controlled temperature and no relative humidity control except by opening windows. Figure 11 shows the “very wet” climate used in the container in order to place maximum hygrothermal stress on the roof specimens. All climate types were used in modelling and developing design graphs, see below.

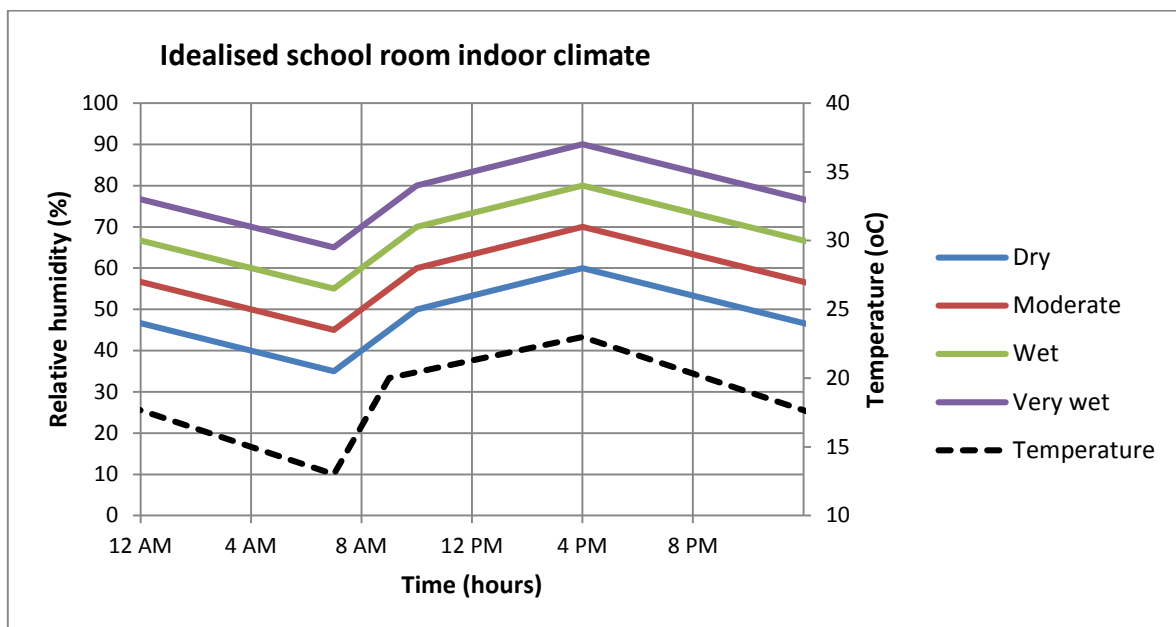


Figure 11: Idealised school room climate used in this study. The “very wet” climate was used in the container. All climate types were used in the modelling.

Control was provided by two convection heaters, a centrifuge humidifier and a dehumidifier. Simple “ON/OFF” control is used. The acquisition software measures, every minute, the

temperature and the relative humidity of the air in the container and decides which device to switch on or off based on a comparison with the corresponding set-point.

5.2 Measurement of air flow characteristics

Ventilation is essential in shaping the hygrothermal environment in roof spaces. Ventilation from outdoors into the roof space and from the indoor condition space into the roof can strongly influence the moisture balance of the air inside the roof space.

In order to gather some insights into the magnitude of the air exchanges in the roof spaces and to complement the temperature and relative humidity measurements, airtightness measurements aimed at determining the air flow characteristics of the roof specimen were conducted. The air flow characteristics are described using the air flow resistances of the various openings around the specimen. The air flow resistance expresses the relationship between pressure differences across the opening and air flow across it. Usually the relationship is modelled in the following way:

$$Q = C |\Delta P|^n$$

where Q is the air flow rate (in m^3/h), ΔP is the pressure difference (in Pa), C is the characteristic coefficient (in $m^3/h Pa^n$) and n is the characteristic exponent. The parameters C and n describe the flow characteristics of the opening. Once C and n have been determined, the average air flow rate through the opening can be estimated by measuring the average pressure difference that exists across the opening under normal weather conditions.

The air flow resistances were measured by means of a calibrated fan and a pressure transducer. The Retrotec Q5E blower door provides automated facilities to easily conduct airtightness measurements of confined spaces. To conduct a test, the fan is usually mounted to just blow air into a well defined space, i.e. the roof space. During a test the in-built pressure transducer measures the pressure difference between the confined space and outdoors and provides a feedback for the controller of the fan motor. The fan is then controlled to constantly maintain the pressure difference. Once the required pressure difference is achieved, the fan controller measures the air flow rate traversing the fan. Because the space is confined and well delimited, the air which is flowing through the fan is also flowing through the openings of the space under examination. By stepping through a series of pressure differences, the characteristic curve Q vs ΔP for the openings of the space can be sampled. A least square fit of these data points then allows computing of the characteristic coefficient and the characteristic exponent for the ensemble of the openings.

Several techniques can be used in order to isolate the air flow characteristic of specific openings of, in our case, the roof space. Four major distributed openings can be identified in the roof specimen: at the eaves, at the ridge, along the sides and at the level of the suspended ceiling. One simple technique to isolate a specific opening is to try and seal all other openings before conducting the measurements using the blower door. With all openings sealed bar one, the air flowing through the fan only moves through the unsealed opening and its air flow characteristics can be determined. The distributed openings along the sides of the roof specimen are always sealed because heat, moisture and air movements from the sides were minimised by design with the introduction of extra insulation and moisture and an airtight membrane. The distributed opening at the ridge can be sealed reasonably easily by sellotaping an airtight membrane along its length.

However, the suspended ceiling cannot be easily sealed off using an airtight membrane. By observing the form of the generic air flow curve, it can be seen that if the pressure difference across an opening can be actively maintained as close to zero as possible, there will be very

little air flow traversing it. This can be achieved by using a second fan to counterbalance the pressure difference generated across the ceiling by the first fan, as shown in Figure 12. When the secondary fan is switched off, the primary fan generates a predetermined pressure difference ΔP_a between the roof space and outdoors. At the same time, it creates a pressure difference ΔP_2 across the suspended ceiling. By switching on the secondary fan, adjusting its speed and monitoring the pressure difference ΔP_2 , the difference in pressure ΔP_2 can be set very close to zero. While manually adjusting the secondary fan, the first fan will automatically adjust its speed to maintain the required pressure difference ΔP_1 .

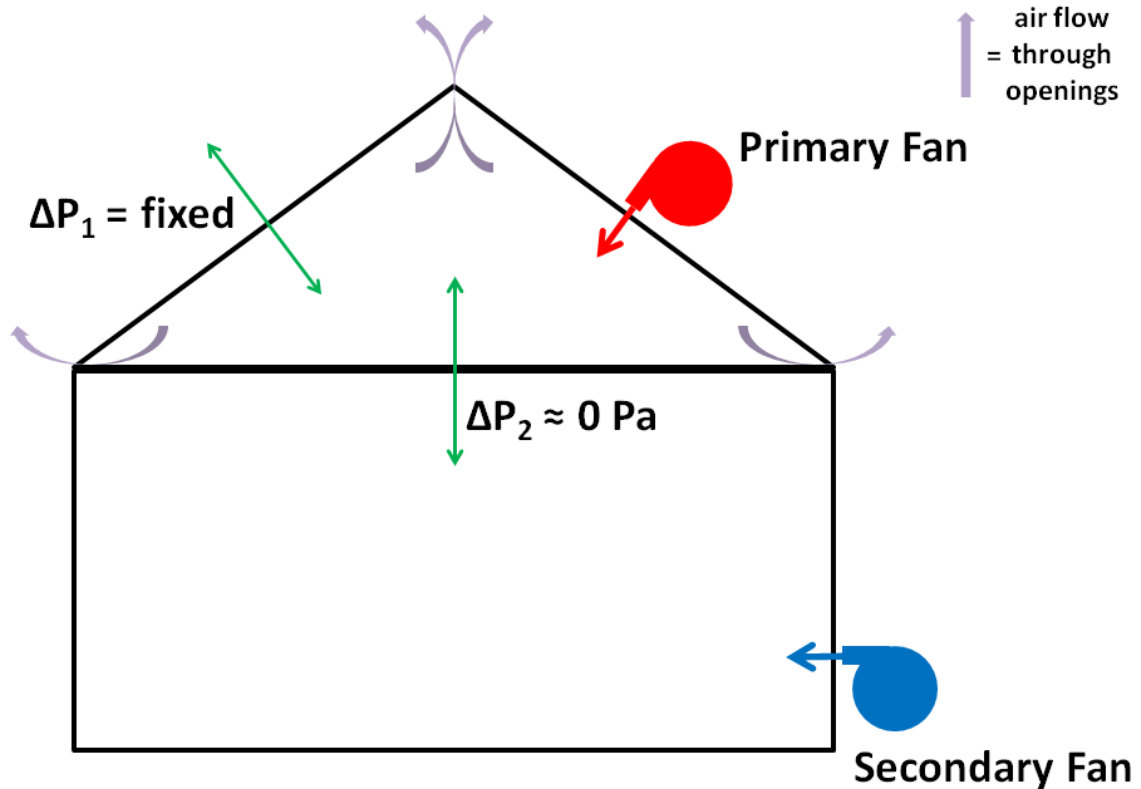


Figure 12: Schematic of a pressurisation test of the roof space where the air flow through the ceiling has been dynamically “cancelled out” by using a second fan to reduce the pressure difference ΔP_2 to zero.

6. RESULTS

Figure 13 shows the psychrometric conditions through each roof specimen at selected times, while Figure 14 to Figure 17 show specimen behaviour over representative time periods.

For the timber roof and, to a lesser extent, for the EPS roof temperatures near the metal purlins are very close or equal to the local dewpoint, and consequently the relative humidities at these locations are very high. The phenolic roof and the bonded panel roof have much lower relative humidities around the timber purlin.

6.1 Phenolic roof

The phenolic roof purlin air conditions close to the metal purlins are dominated by indoor conditions with the temperature lagging room temperatures by around an hour, the relative humidity lagging the room relative humidity by a few hours and the vapour pressure lagging room vapour pressure by a quarter-hour at most. Some outdoor influence can be seen though; notice that on the 8/7/12 when the outdoor temperature and relative humidity show only small diurnal variations there is also some truncating of the amplitude of the purlin temperatures and humidities.

6.2 Timber roof

Purlin air temperatures, relative humidities and vapour pressures are set by outdoor conditions with no indoor influence visible. This can be seen clearly in the period between 12/8/12 and 15/8/12 where outdoor conditions nearly constantly lead purlin temperatures and relative humidities with no influence from indoor conditions. Purlin air temperatures lag outdoor temperatures by around half an hour, relative humidities lag just a little longer and vapour pressures show little phase difference.

6.3 EPS roof

The EPS structure conditions are controlled mostly by outdoor conditions. This can be seen in Figure 16 during the period 20/8/12 to 21/8/12 where outdoor conditions are nearly constant. As a result, the purlin air temperature peak to peak amplitude falls from around 8°C to around 1.5°C, the relative humidity amplitude falls by 27% to around 5% and the vapour pressure amplitude falls by 450 Pa to 150 Pa. These lower amplitude levels allow a residual response to indoor conditions to become visible which is about a third of the total level, implying that the outdoor to indoor climate influence is about two to one. This is consistent with the modelling below. Purlin air psychrometric conditions lag the indoor temperature by negligible amounts.

6.4 Metal panel roof

The peak purlin relative humidity is set by the outdoor relative humidity with a phase lag of one or two hours. At 11:45 am on the 15/9/12, it can be seen that while the outdoor relative humidity has dropped from 97% to 80%, the purlin relative humidity falls by only 1%, despite the indoor relative humidity still falling to 64% later in the day, confirming that the purlin relative humidity is dominated by the outdoors humidity. Vapour pressures are found to follow the same trend.

Purlin air relative humidity mostly follows outdoors with a large phase lag of one-and-a-half to two hours, but although the purlin air relative humidity has only a very small response to the indoor relative humidity, this small response is immediate.

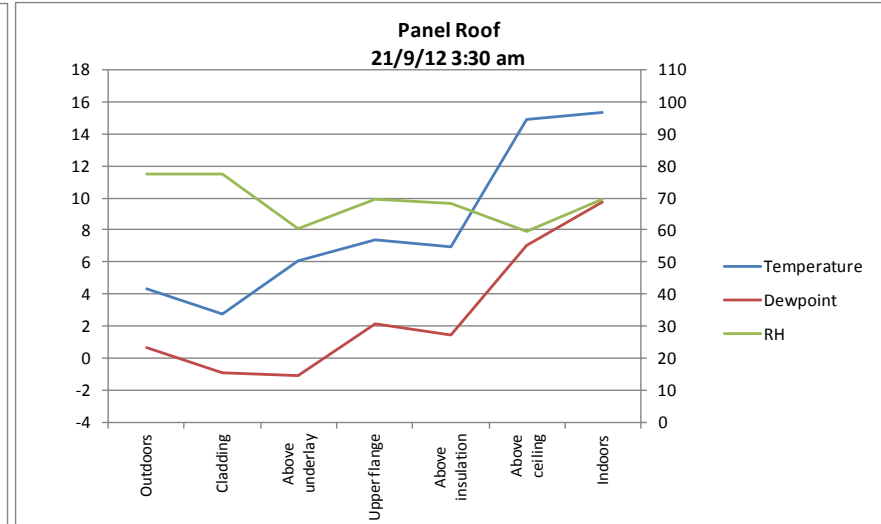
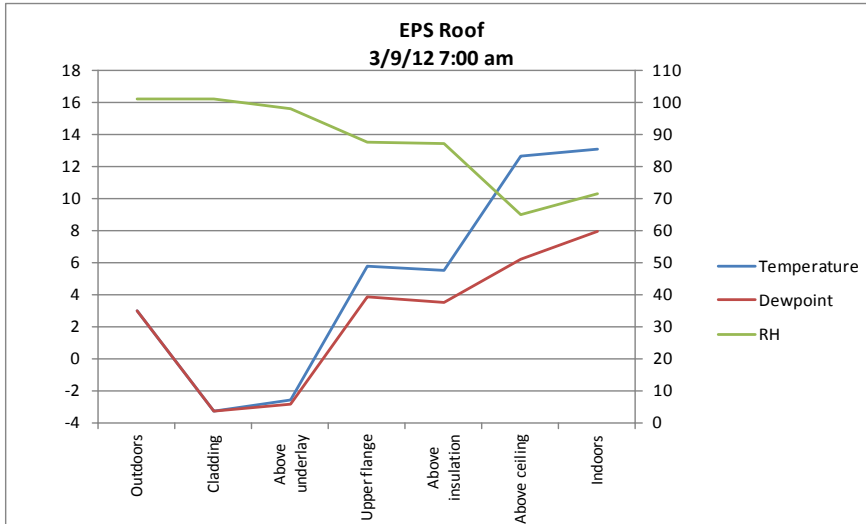
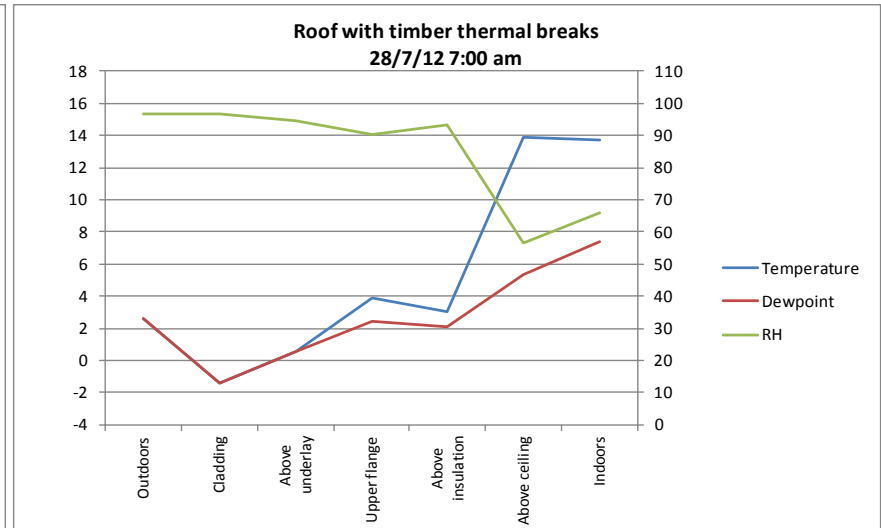
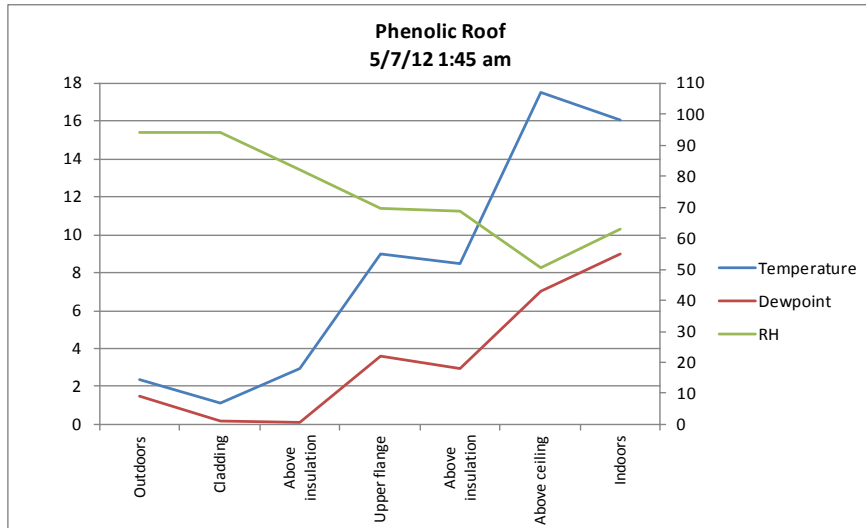


Figure 13: Cross sections through the roof at selected times (horizontal axis categorical, i.e. not scaled).

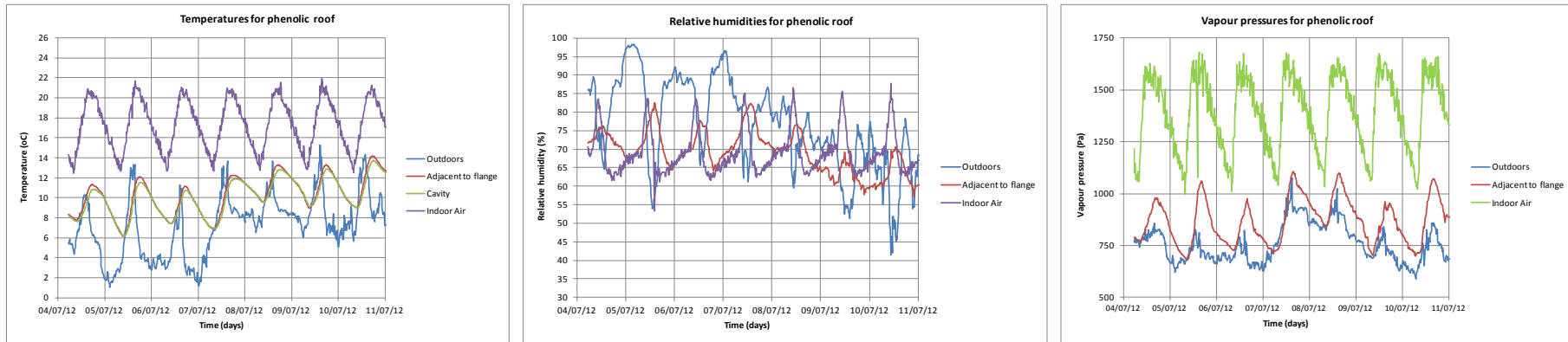


Figure 14: Psychrometric conditions for representative periods for the purlin air of the phenolic specimen.

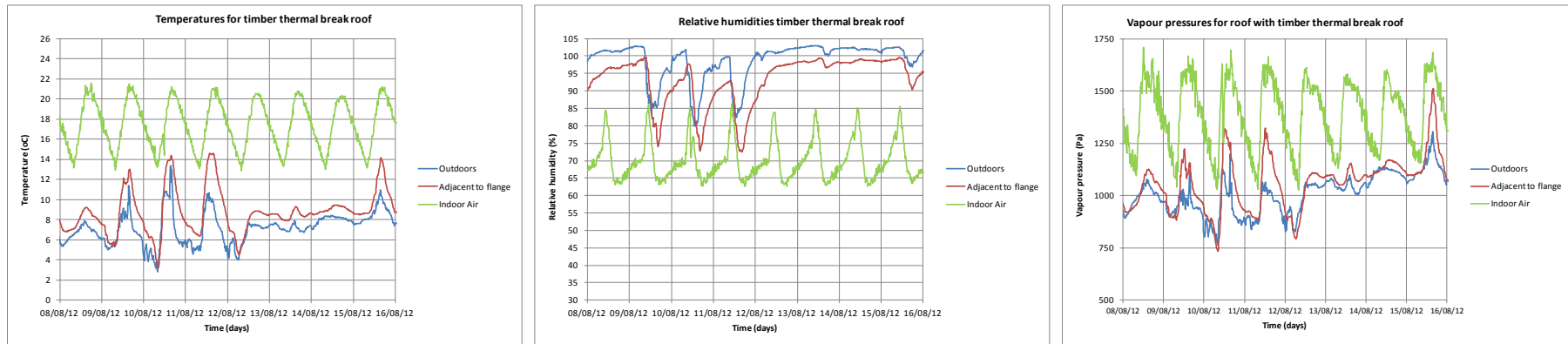


Figure 15: Psychrometric conditions for representative periods for the air adjacent to the purlin of the timber specimen.

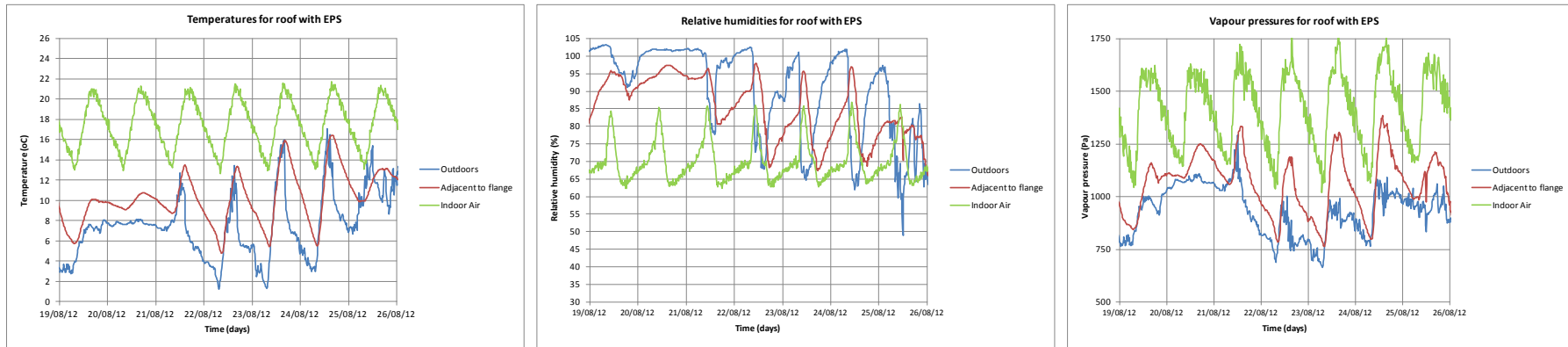


Figure 16: Psychrometric conditions for representative periods for air adjacent to the purlin of the EPS specimen.

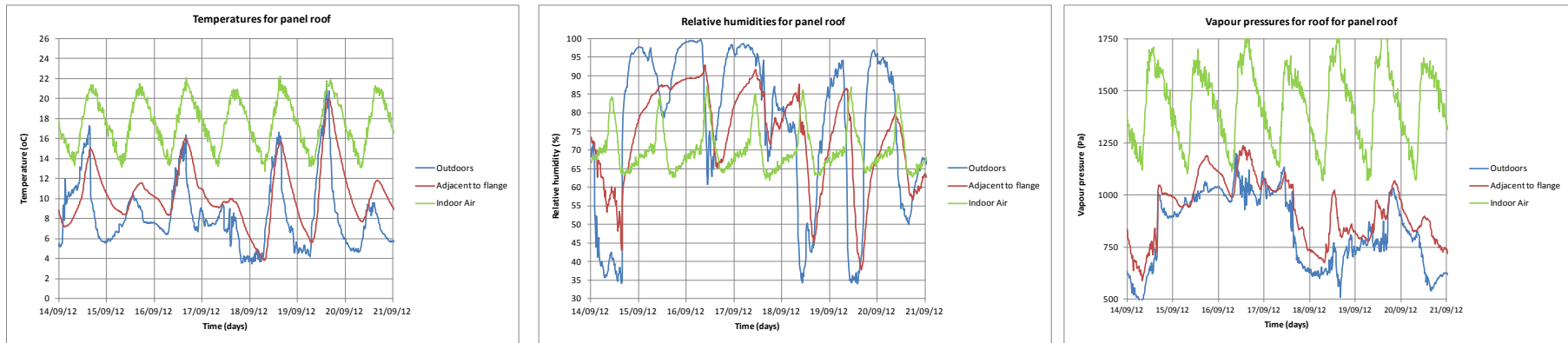


Figure 17: Psychrometric conditions for representative periods for air adjacent to the purlin of the panel specimen.

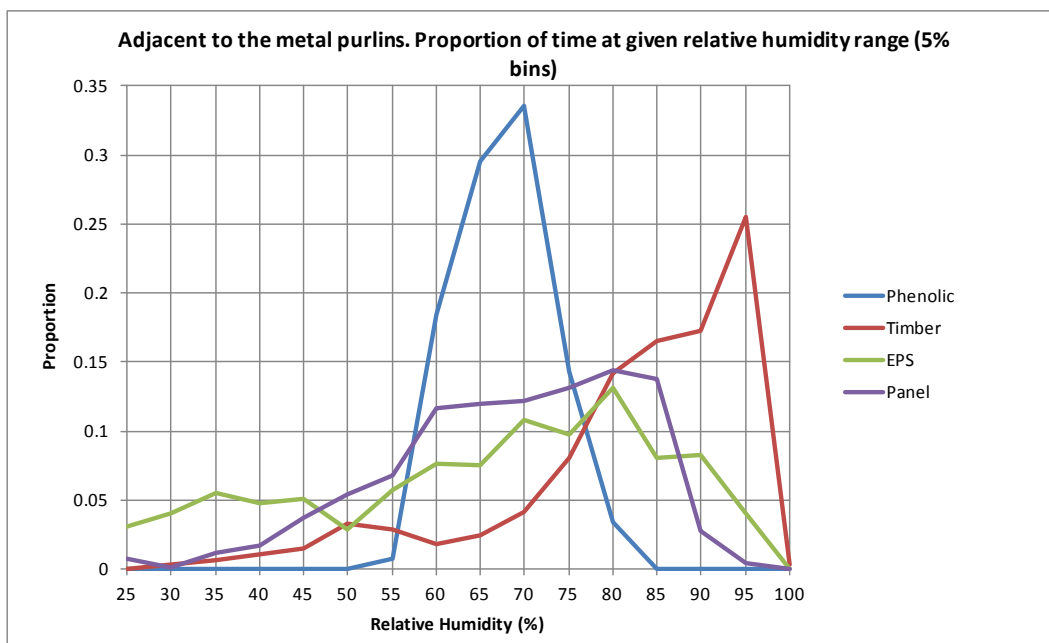


Figure 18: Histogram of relative humidities of the air adjacent to the metal purlins (includes rain events).

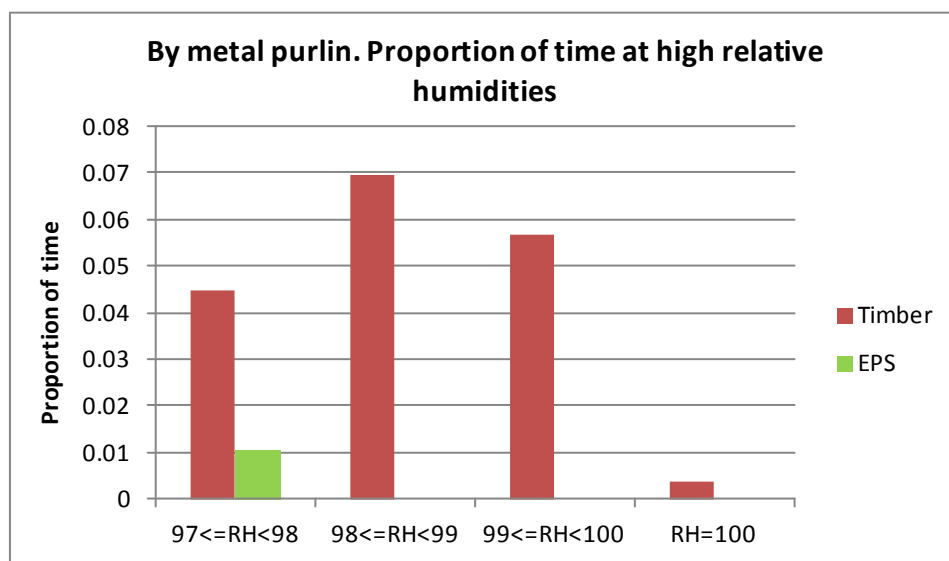


Figure 19: Histogram of high relative humidities of the air adjacent to the metal purlins for roofs with timber and EPS roofs (includes rain events).

6.5 Condensation events

We make the definition that: while relative humidities are above 98% there is a condensation event.

However, in making the condensation episode definition we need to distinguish them from rain events. For the timber roof there was a significant episode of very high relative humidities in the air adjacent to the purlin over a period of 38 hours from 13/8/12 2015 15 hours to 15/8/12 1015 hours. During this time the associated temperature was confined to a range of 6.6°C to 9.2°C in response to an identical outdoor temperature within 0.5°C. This was an extensive rainy episode confirmed by climate files cliflo.niwa.co.nz with our outdoor relative humidity

sensors showing relative humidity at 100% throughout the time period. There was another significant rainfall event on 31/7/12.

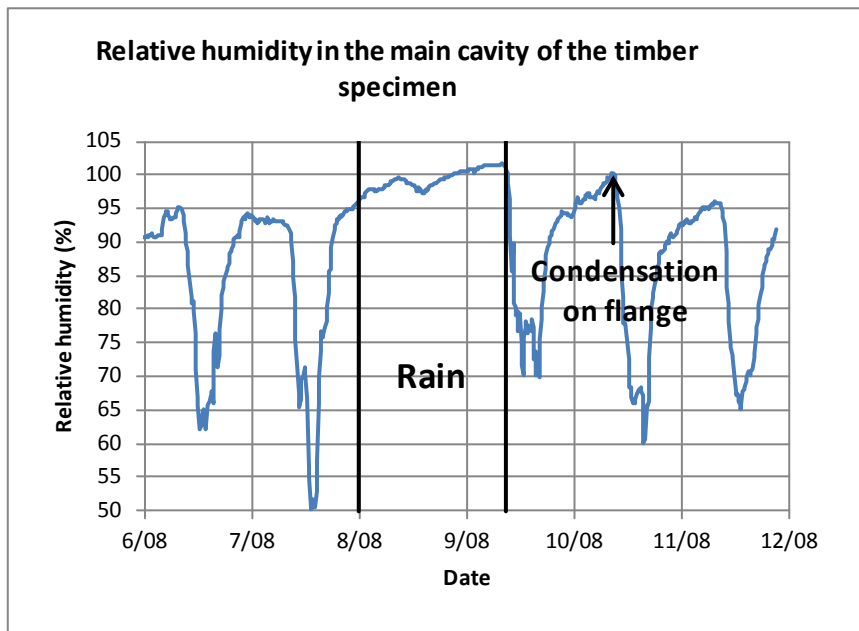


Figure 20: A condensation episode happens on the purlin flange the morning after a period of rain.

For the timber specimens there is a condensation event associated with every rain period. As illustrated in Figure 20 these specimens show condensation the morning after the rain event, after sunrise as the roof is heating up. The mechanism here is that the timbers of the specimen absorb moisture from the 100% humidity air in the cavity during rain and discharge this excess moisture when the timbers are heated up the next morning, giving rise to a condensation event. For the other specimens the cavity air does not rise to such high relative humidities during rain and the discharge humidities next morning are also relatively low.

Figure 18 to Figure 22 summarise the ranges of relative humidity experienced by each specimen. It was found that, for air adjacent to the metal purlins, only the timber thermally broken roof has condensation events and that the EPS roof is close to condensation event level with relative humidities between 97% and 98%.

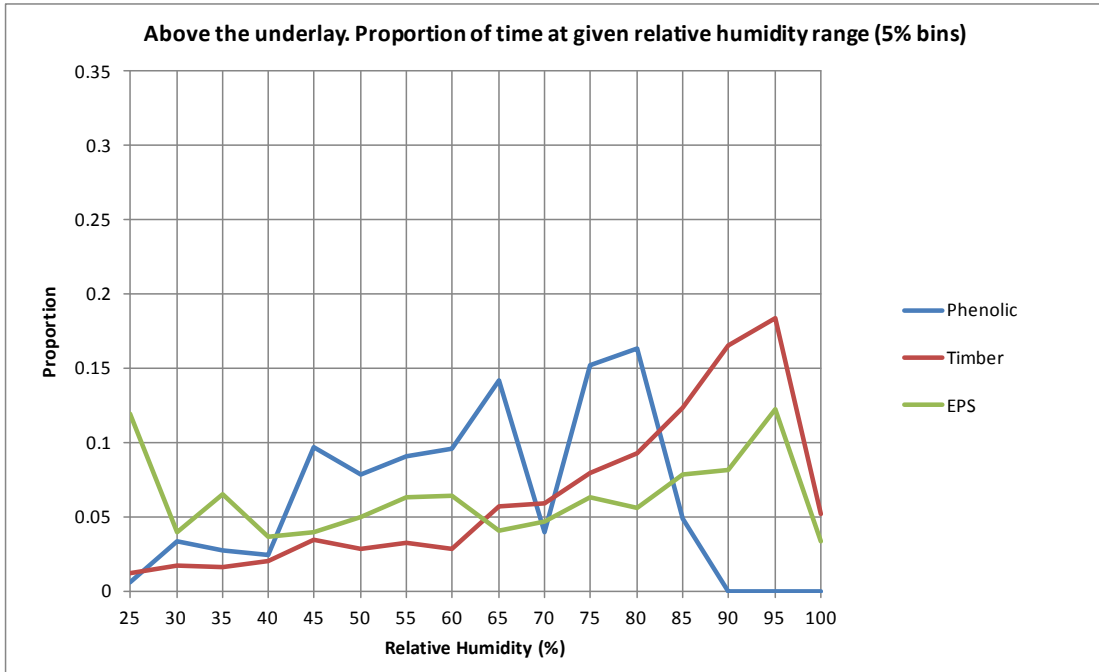


Figure 21: Histogram of relative humidities of the air in the small cavity above the underlay and below the cladding (includes rain events).

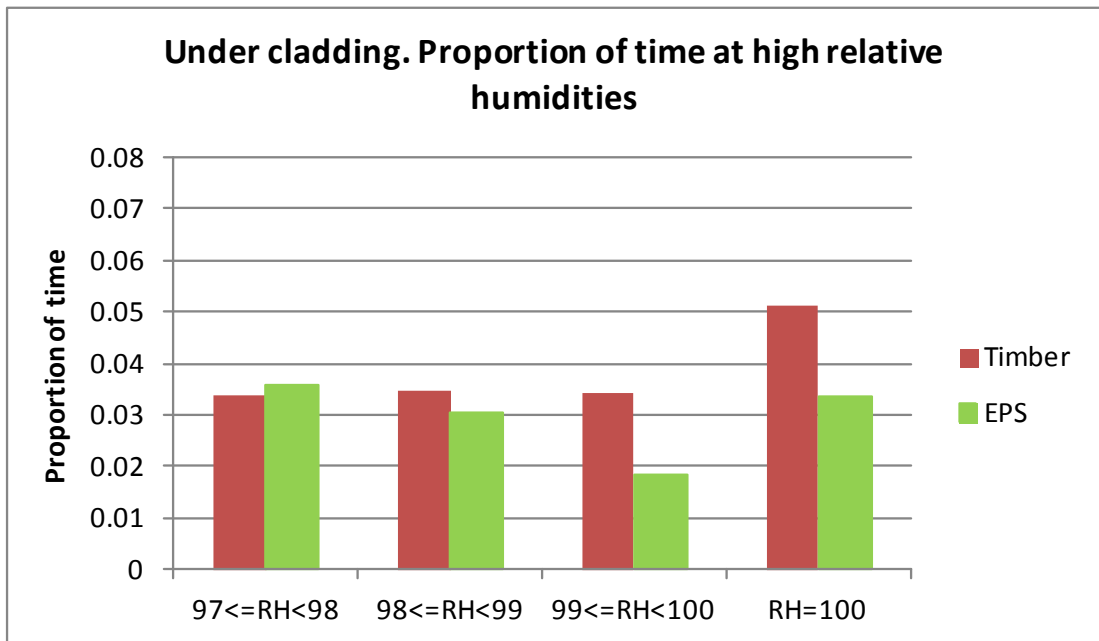


Figure 22: Histogram of high relative humidities of the air in the small cavity above the underlay and below the cladding, for timber and EPS roofs (includes rain events).

	Dates of observations	By metal purlin		Above underlay	
		Percent of time high relative humidity associated with rain	Percentage of time high relative humidity associated with condensation	Percent of time high relative humidity associated with rain	Percentage of time high relative humidity associated with condensation
Phenolic roof	15/06/2012-10/07/2012	0%	0%	0%	0%
Timber thermal break roof	13/07/2012-15/07/2012	11.6%	1.4%	6.6%	5.4%
EPS roof	18/07/2012-11/09/2012	0%	0%	3.3%	5.0%
Panel roof	14/09/2012-15/10/2012	0%	0%	0%	No underlay

Table 1: Prevalence of condensation events.

For the EPS roof there was just one condensation event, on 22/8/12 between 10:15 and 11:00 am. In total, condensation happened just 0.004% of time that the roof was studied. These results are summarised in Table 1. Some of the data in Table 1 is due to the change in climate going from the middle of winter to late winter.

6.6 No night condensation events

The fact that there was no condensation through the night even for the timber specimen was unexpected and requires some explanation.

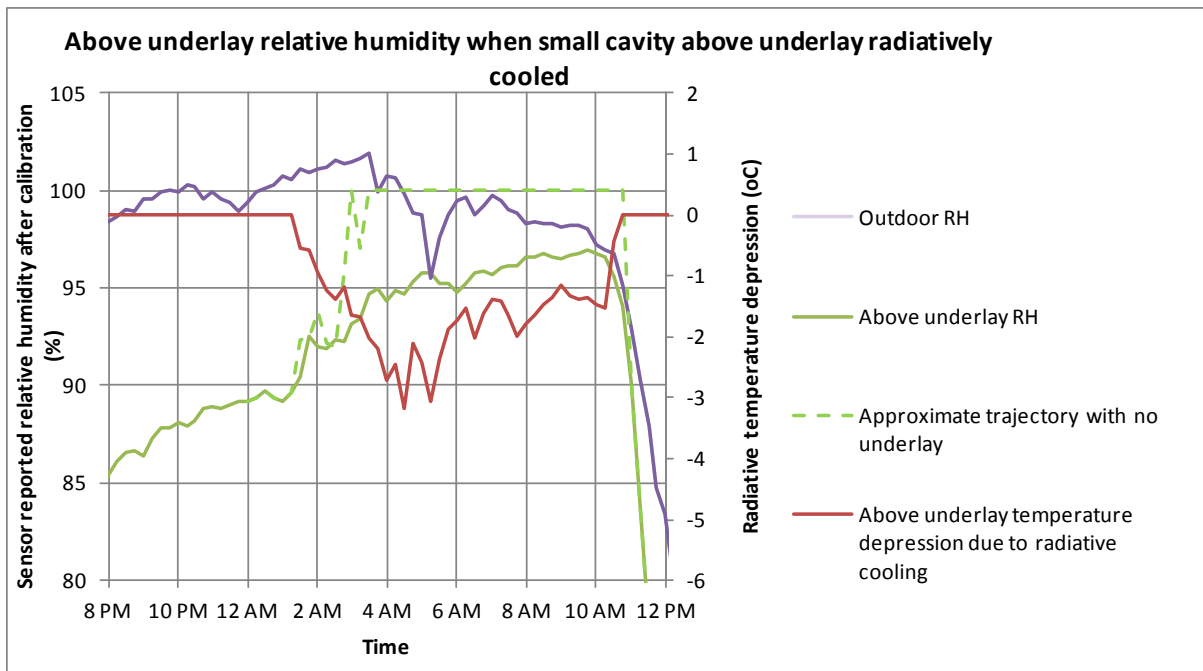


Figure 23: Above underlay relative humidity when small cavity above underlay radiatively cooled (phenolic specimen).

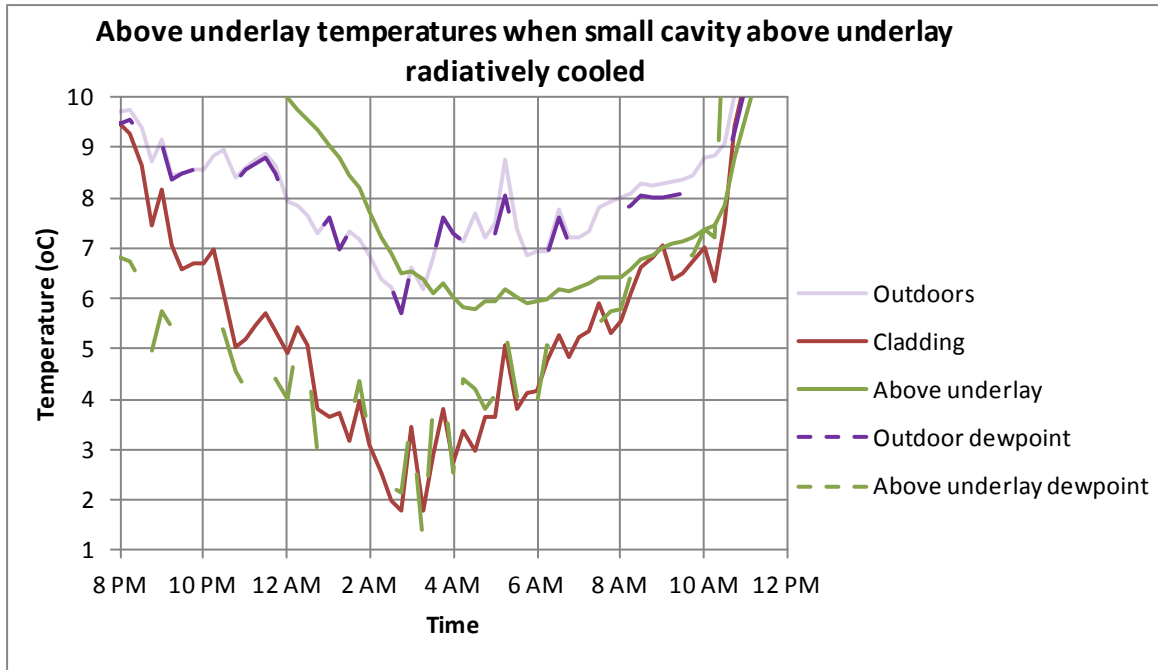


Figure 24: Above underlay temperatures when small cavity above underlay radiatively cooled (phenolic specimen).

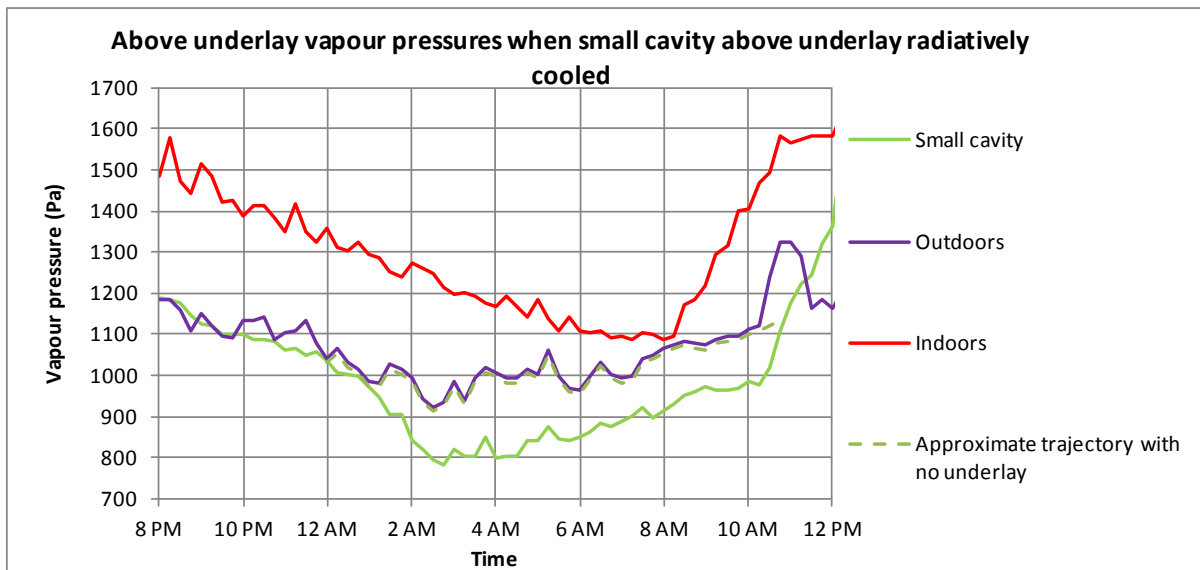


Figure 25: Above underlay vapour pressures when small cavity above underlay radiatively cooled (phenolic specimen).

When the metal roof radiates its heat away into the cold sky during frosty nights its temperature falls significantly below the outdoor temperature and often also below the ambient dewpoint. As a consequence condensation or frost forms on the top of the metal roof.

Under these conditions the small cavity above the underlay also falls to very low temperatures. The air in this small cavity is a mixture of outdoor and indoor sourced air so its vapour pressure could be expected to be at least as large as the outdoor air vapour pressure, and therefore its dewpoint to be at least as high as the dewpoint of the outdoor air. If this is so, condensation should take place on the underside of the cladding.

However, that does not happen.

The reason being that the underlay exerts hygroscopic control on the small cavity above it absorbing vapour from it to maintain an equilibrium between the underlay relative humidity and the cavity relative humidity, as can be seen in Figure 23.

Consequently the cavity vapour pressure drops below the trajectory that would be expected from examining indoor and outdoor vapour pressures, see Figure 25. The cavity temperature, although well below the outdoor dewpoint, is well above the cavity dewpoint. This mechanism has been anticipated by Cunningham and Quaglia in their modelling of the moisture performance of underlay under roofs [13].

This is a significant result as it solves the mystery of why condensation or frosting is observed on the top of the metal cladding but not the bottom. The assumption, now shown to be incorrect, has always been that the dewpoint of the small cavity air is at least as high as the outdoor air, implying that if there is condensation or frosting on the on the top of the metal cladding then there is condensation or frosting on the under surface of the metal cladding.

The result is also significant in that it highlights the fact that one of the functions of a hygroscopic underlay is to prevent or lessen the amount of condensation on the under surface of the metal cladding.

6.7 Measurement of air flow characteristics

The air flow characteristics of the main openings of the roof specimen were determined by a series of fan pressurisation tests.

The first test (Figure 26) consisted in the pressurisation of the container supporting the roof specimen. These measurements resulted in the following air flow characteristic curve:

$$Q[m^3/h] = 102.5 |\Delta P|^{0.6891}$$

where the pressure difference ΔP [Pa] is between the indoor of the container and outdoor. This air flow characteristic described the combined contribution of air flow through the suspended ceiling and through distributed openings along the walls of the container.

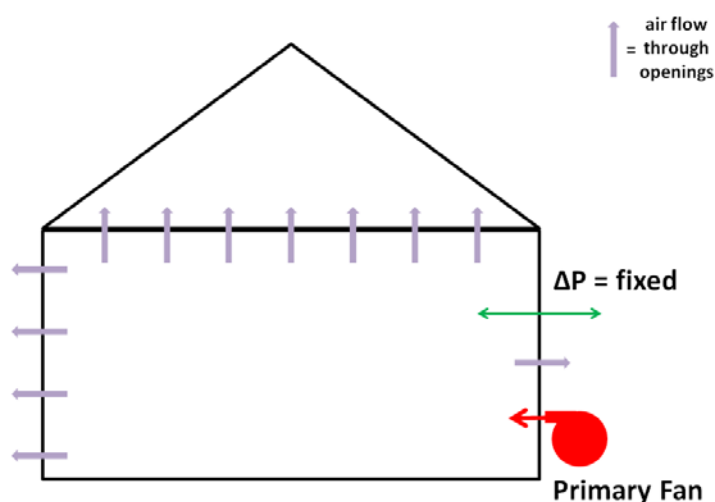


Figure 26: Schematic of a pressurisation test of the container space.

For the second test (Figure 27) the walls of the container were lined with an airtight membrane in order to seal off the distributed openings along the walls. The container was pressurised and the pressure difference across the suspended ceiling was measured giving the following air flow characteristic:

$$Q[m^3/h] = 73.5 |\Delta P|^{0.6817}$$

where the pressure difference $\Delta P [Pa]$ is across the ceiling (ΔP_2 in Figure 27). This air flow characteristic describes the permeability of the suspended ceiling for an upwards air flow. This test leads to a relationship between the pressure difference between the indoor of the container and outdoor (ΔP_1) and the pressure difference across the ceiling (ΔP_2). The relationship is linear:

$$|\Delta P_2| = 0.743 |\Delta P_1|$$

Combining these three relationships, the air flow characteristic of openings along the walls of the container can be determined as:

$$Q[m^3/h] = 42.5 |\Delta P|^{0.6990}$$

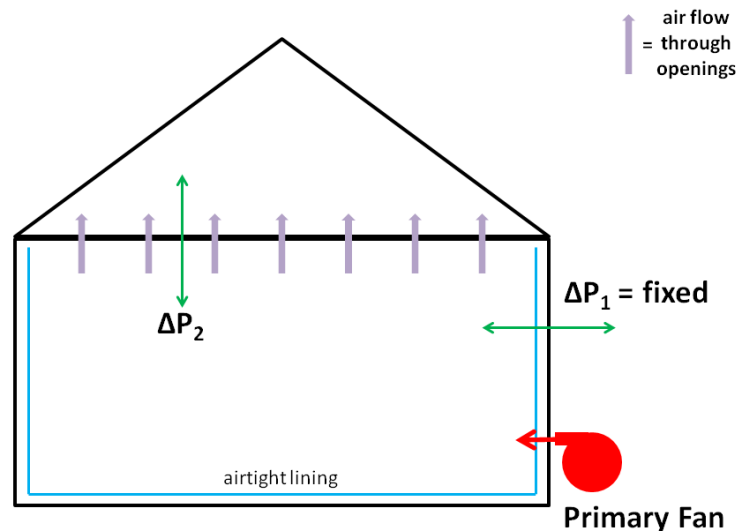


Figure 27: Schematic of a pressurisation test of the container space after lining its walls with an airtight layer.

The third test (Figure 28) consisted of the pressurisation of the roof space. The door of the container was left open in order to ensure that pressure across all the boundaries of the roof specimen was the same. The measurements resulted in the following air flow characteristic:

$$Q[m^3/h] = 166 |\Delta P|^{0.7388}$$

where the pressure difference $\Delta P [Pa]$ is across the indoor of the roof space and outdoor. This air flow characteristic described the combined contribution of air flow through the suspended ceiling and through distributed openings along the eaves of the roof specimen (the ridge was sealed).

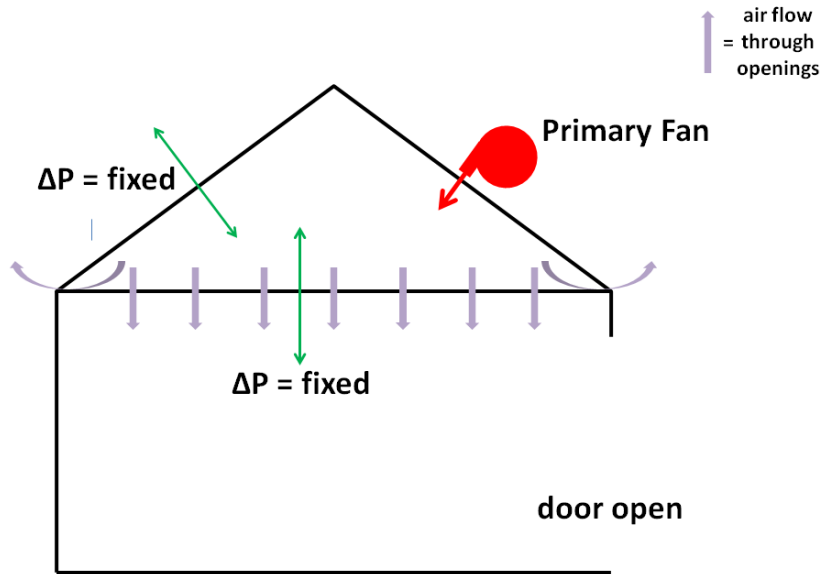


Figure 28: Schematic of the pressurisation test of the roof space.

The fourth test (Figure 29) was similar to the third, but a second fan was mounted on the door in order to reduce to zero the pressure across the suspended ceiling. The air flow characteristic obtained in this way was:

$$Q[m^3/h] = 156 |\Delta P|^{0.5081}$$

where the pressure difference $\Delta P[Pa]$ is across the indoor of the roof space and outdoor. This air flow characteristic described the flow through the eaves of the roof specimen (the ridge was sealed).

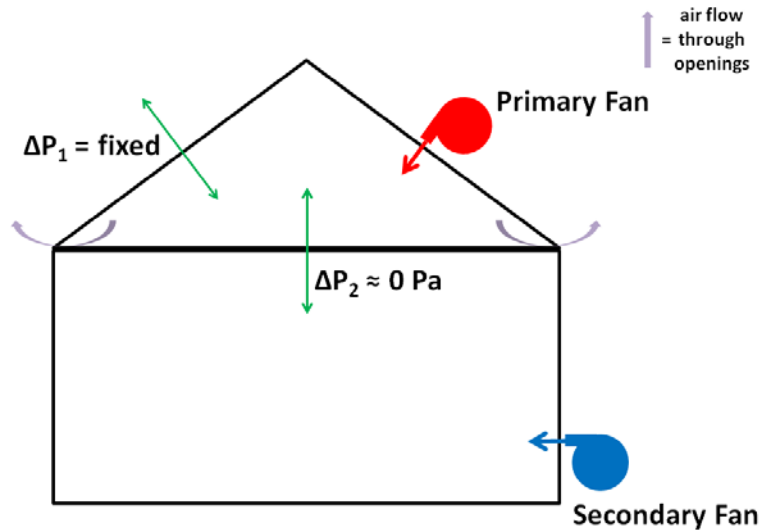


Figure 29: Schematic of the pressurisation of roof space with air flow through the ceiling cancelled out by means of a second fan.

Subtracting the last two relationships, we obtain the air flow characteristic of the suspended ceiling for air flow going downwards:

$$Q[m^3/h] = 49 |\Delta P|^{0.9318}$$

All the experimental results presented in this section are summarised in Table 2.

FLOW CHARACTERISTICS	Q = C ΔP ⁿ	
	C	n
of	[m ³ /(h Pa ⁿ)]	[-]
Container (walls + ceiling)	102.5	0.6891
Container (walls only)	42.5	0.6990
Roof (eaves + ceiling)	166	0.7388
Roof (eaves only)	156	0.5081
Ceiling (flow upwards)	73.5	0.6817
Ceiling (flow downwards)	49	0.9318

Table 2: Air flow characteristics of various (distributed) openings in the roof specimen and in the container

6.8 Estimation of ventilation rates

The average air flows through the different openings of the roof specimen and the container can be estimated from the various air flow characteristics and from the average pressure differences across them. Figure 31 shows an example of pressure difference between the indoor of the roof space and outdoor, and between the indoor of the container and outdoor, during a windless and cloudless night. The average pressure differences are quite minute but the pressure gauge is sufficiently accurate to be able to resolve them. The average pressure differences are 1.15 Pa for the roof space, 1.05 Pa for the indoor of the container and 0.1 Pa across the ceiling. The difference in these means taken from Figure 31 is highly significant statistically ($p < 0.001$).

Figure 32 summarises the resulting air flow rates computed by putting together the various air flow characteristics and average pressure differences. Considering the volumes of the different spaces, the average ventilation rate through the roof space is around 15 ach (air changes per hour), the one through the container 0.5 ach and the one through the ceiling around 5 m³/h. Taking into account the volume of the roof space, this last air flow rate corresponds to around 0.5 ach.

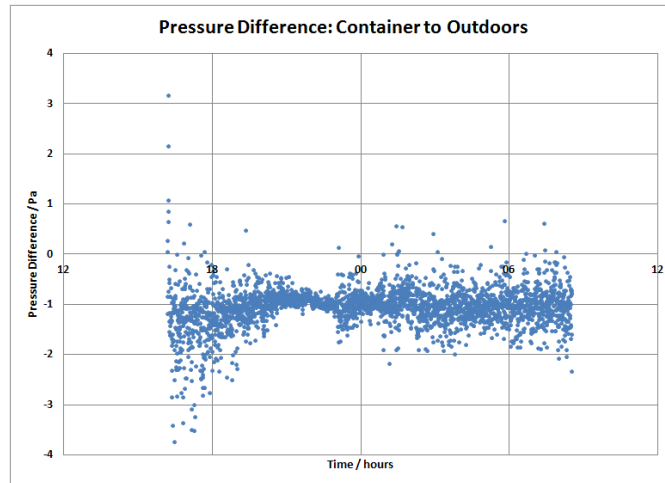


Figure 30: Example of pressure differences between container space and outdoors during a calm and cloudless night.

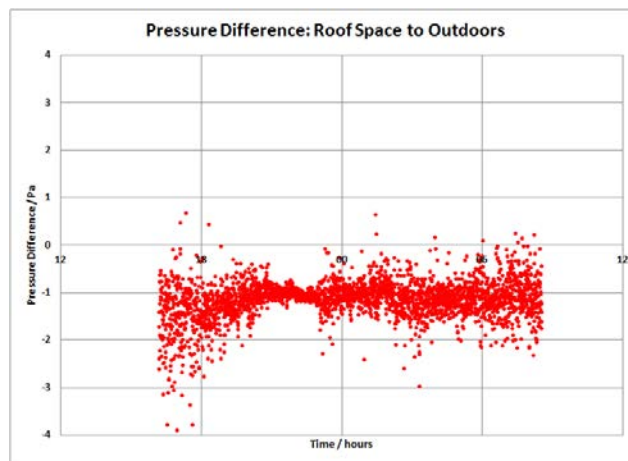


Figure 31: Example of pressure differences between roof space and outdoors during a calm and cloudless night.

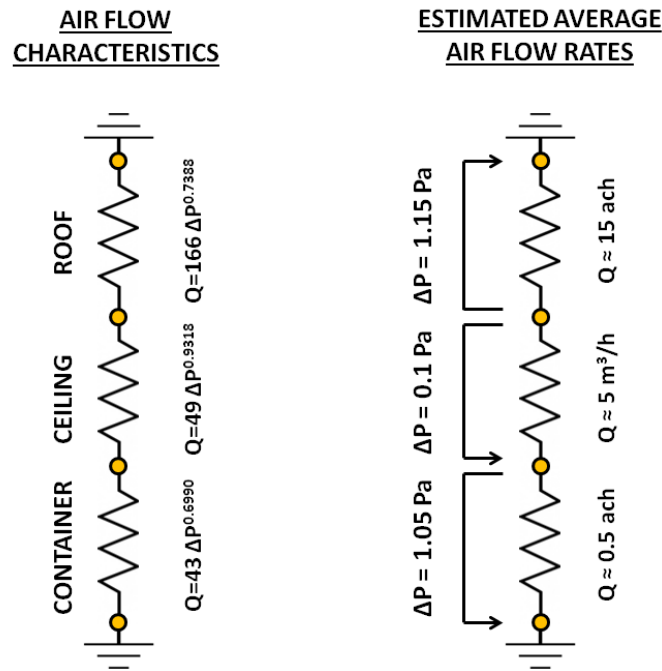


Figure 32: Very simplified equivalent resistance network schematising the air flow resistances between container space and outdoor, between roof space and outdoor, and across the ceiling.

6.9 The relative importance of ventilation, diffusion and hygroscopic moisture fluxes

The flux of moisture into and out of the specimen cavities is determined by ventilation levels and the size of the lining and cladding diffusive resistances.

We have:

$$\begin{aligned}
 Q_{ceiling} &= Q_a + Q_d \\
 &= F_{ic}V(c_i - c_c) + \frac{A_c}{r_c}(p_i - p_c) \\
 &= \left(\frac{F_{ic}VW}{RT} + \frac{A_c}{r_c} \right) (p_o - p_c) \quad (1)
 \end{aligned}$$

where small density changes in the air as it moves into regions with different temperatures is ignored. F_{ab} is the air change rate from location a to location b (s^{-1}), c_c is the vapour concentration ($kg\ m^{-3}$) a cavity c , c_o is the vapour concentration in the indoors or outdoors. (Other terms in the Nomenclature at the beginning of the report). There is a similar formula for outdoor-cavity moisture fluxes.

We define a dimensionless number C_e which is the ratio of the ventilation and diffusion fluxes, so from equation (1):

$$C_{e_{indoor}} = \frac{Q_v}{Q_d} = \frac{F_{ceiling} r_{ceiling} VW}{ART} \quad (2)$$

with a similar formula for $C_{e_{outdoor}}$ for flow from outdoors. However, for the outdoor case we have zero diffusive flow through the metal roof so that $C_{e_{outdoor}}$ is infinity.

Values for C_e for the main cavity for all specimens are given in Table 3.

Air change rate (h^{-1})	C_e Ratio of ventilative to diffusive fluxes
1	4.4
10	44
20	89

Table 3: $C_{e_{ceiling}}$, the ratio of ventilative to diffusive fluxes in the main cavity of all specimens. $C_{e_{outdoor}}$ is infinite.

Air change rate (h^{-1})	C_e Ratio of ventilative to diffusive fluxes		
	Phenolic	Timber	EPS
10	640	2.9	23
50	3200	15	120
100	6400	29	230

Table 4: $C_{e_{indoor}}$, the ratio of ventilative to diffusive fluxes in the cavity below the cladding (no cavity for the metal panel specimen). $C_{e_{outdoor}}$ is infinite.

All C_e values are considerably higher than 1 which means for ventilation rates greater than a few air change per hour, diffusion has negligible effect on cavity moisture contents.

Similarly Table 4 gives the value of C_e for the small cavity immediately below the cladding and above the underlay. In the case of the metal panel specimen, the underlay sits hard up against the underside of the panel so this small cavity does not exist.

Moisture is transferred in and out of hygroscopic materials under periodic relative humidities. Under these conditions moisture appears to be concentrated at a point at an effective depth within the material given $d_{eff} = \sqrt{\frac{D}{2\omega}}$ through an effective resistance of $r_{eff} = \frac{d_{eff}}{D} + r_s$, see [14], where D is the diffusion coefficient for moisture transfer with moisture content as the driving potential ($m^2 s^{-1}$), ω is the frequency, daily in this case, and r_s is the surface mass transfer resistance. For daily cycles in timber, r_{eff} is around $1.8 \times 10^7 s m^{-1}$ for wood for moisture content driving potential which is equivalent to $1.8 \times 10^8 MNs/g$.

We define a dimensionless number C_i given by the ratio of ventilative to hygroscopic fluxes and similarly to equation (2) we find:

$$C_i = \frac{Q_v}{Q_h} = \frac{Fr_{eff}VW}{ART} \quad (3)$$

	Phenolic	Timber	EPS	Panel
Area of timber facing the main cavity (m ²)	0.6	0.18	0	0
Air change rate (h ⁻¹)	C _i Ratio of ventilative to hygroscopic fluxes			
1	0.29	0.97	Infinity	Infinity
10	2.9	9.7	Infinity	Infinity
20	5.8	19.5	Infinity	Infinity

Table 5: C_i, the ratio of ventilative to hygroscopic fluxes in the main cavity of each specimen.

Air change rate (h ⁻¹)	C _i
1	0.0014
10	0.014
100	0.143

Table 6: C_i, the ratio of ventilative to hygroscopic fluxes in the cavity below the cladding of each specimen (cavity of all specimens the same size, no cavity for the metal panel specimen).

Values for C_i for the main cavity and the cladding cavity are given in Table 5 and Table 6.

Table 5 shows that once ventilation rates are above a few ach, the hygroscopic materials have no effect on the main cavity air moisture content. For the small cavity below the cladding, on the other hand, we can see in Table 6 that C_i values are very low out to very high air change rates. This implies that the hygroscopic materials in the cavity, viz the underlay, are dominant in determining cavity moisture behaviour. This hygroscopic underlay dominance inhibits the formation of condensation under the metal cladding as can be seen in Figure 25 and is discussed above.

Measurements of the ceiling air leakage rates suggest that they are frequently above this value, suggesting that ventilation from indoors will usually exceed vapour diffusion.

Hence both the external and internal ventilation dominates the performance of these structures and vapour diffusion is a secondary consideration. To understand the performance of these structures requires knowledge of the structures' ventilation levels.

7. MODELLING

Temperature, which is essentially independent of ventilation levels, was modelled using WUFI-2D [12]. Very good fits are obtained for temperature; see for example Figure 33 and Figure 33.

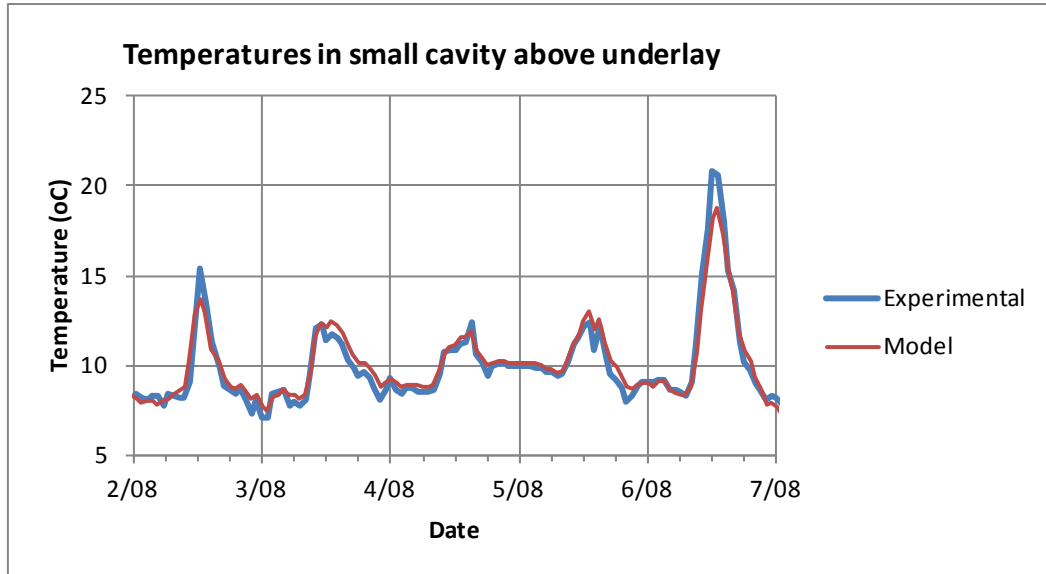


Figure 33: Temperatures in small cavity above underlay for the timber specimen.

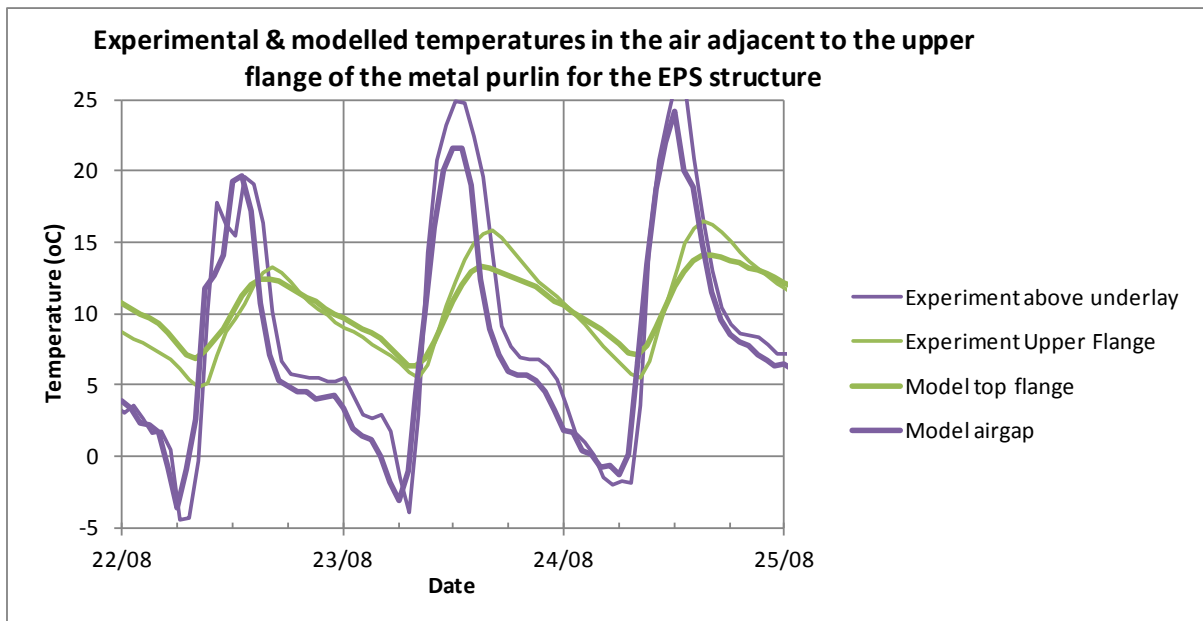


Figure 34: Experimental and modelled temperatures in the air adjacent to the upper flange of the metal purlin for the EPS structure.

To model the effect of ventilation we invoked the fact that ventilation exceeded diffusion and hygroscopic by far in these specimens, i.e. C_e and C_i are large, see Table 4 and Table 5, allowing us to calculate, at each time step, the cavity vapour pressure as the steady-state value that is arrived at given indoor and outdoor vapour pressures, i.e.:

$$\begin{aligned}
 p_c &= \frac{F_o p_o + F_i p_i}{F_o + F_i} \\
 &= \frac{F_o}{F_o + F_i} p_o + \frac{F_i}{F_o + F_i} p_i \\
 &= \alpha p_o + (1 - \alpha) p_i \quad (4)
 \end{aligned}$$

where the *ventilation fraction* α is defined as:

$$\alpha = \frac{F_o}{F_o + F_i}$$

To use equation (4) requires information on air change rates which were not measured during the specimen runs. Hence for the time range of data one is interested in α has been taken as an adjustable parameter, adjusted to give best fit between experimental and modelled cavity relative humidity. With this process a very good standard of fit can be achieved, see for example Figure 35.

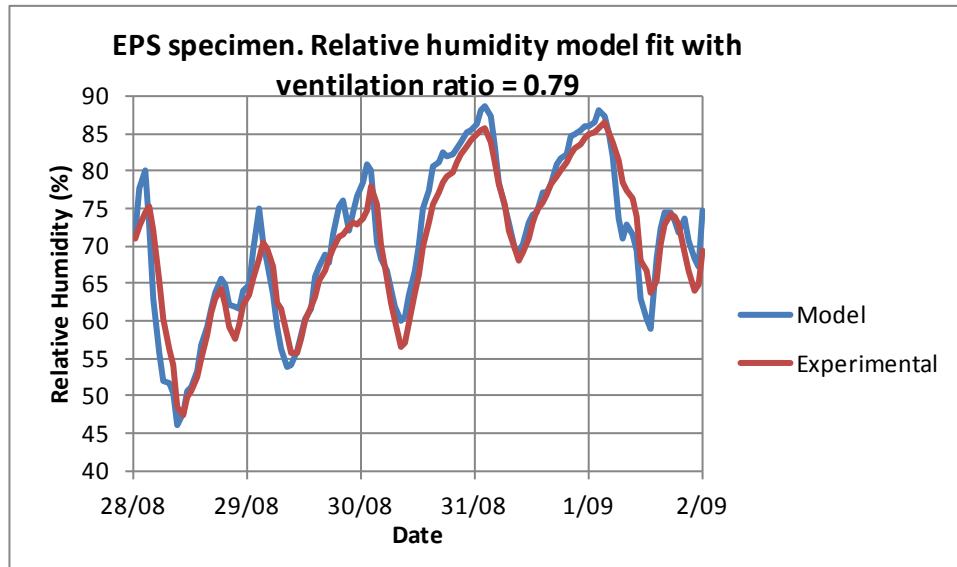


Figure 35: Fitting the relative humidity for the EPS specimen by putting ventilation fraction to 0.79.

8. DESIGN

The main factors determining these roofs' hygrothermal performance are: the roof type; indoor and outdoor climates, i.e. the loadings; the amount of insulation; and the ventilation levels. To size these factors, the performance of each roof over a range of these factors was modelled as detailed above.

8.1 Roof type

The roof types used in the experimental work, with the exception of the timber specimen, all contained rigid insulation systems across the main cavity and purlins of the specimen.

8.2 Loadings

An indoor climate was used simulating in broad terms the indoor climates found in school classrooms where heating is intermittent and no attempt is made to control humidity beyond opening windows. This climate was made up as a set of piecewise line segments of the form:

$$T(t) = T_1 + (t - t_1) \frac{T_2 - T_1}{t_2 - t_1}$$

Climate description	RH_1 7:00 am	RH_2 10:00 am	RH_3 4:00 pm	T_1 7:00 am	T_2 9:00 am	T_3 4:00 pm
Dry	35%	50%	60%	10 °C	20 °C	23 °C
Moderate	45%	60%	70%			
Wet	55%	70%	80%			
Very wet	65%	80%	90%			

Table 7: Indoor climate parameters.

This idealised climate is detailed in Table 1 and illustrated in Figure 11.

The outdoor climate was taken as the Dunedin late winter climate from 18/8/12 to 9/9/12.

8.3 The amount of insulation

Each specimen was modelled with 200 mm of fibreglass insulation on top of the ceiling. The timber specimen was given no further insulation; rigid insulation systems were modelled with R-values of 0.75, 2.25 and 4.5 m² °C/W.

8.4 Ventilation levels

In line with experimental measurements, total roof ventilation was taken as at least 1 ach, allowing diffusion and hygroscopic performance to be ignored when determining main cavity psychrometric conditions. The critical parameter then becomes the ratio of the outdoor ventilation rates to the indoor ventilation rates or what amounts to the same thing, the ratio of the outdoor ventilation rate to the total ventilation rate, which we are calling the "ventilation fraction".

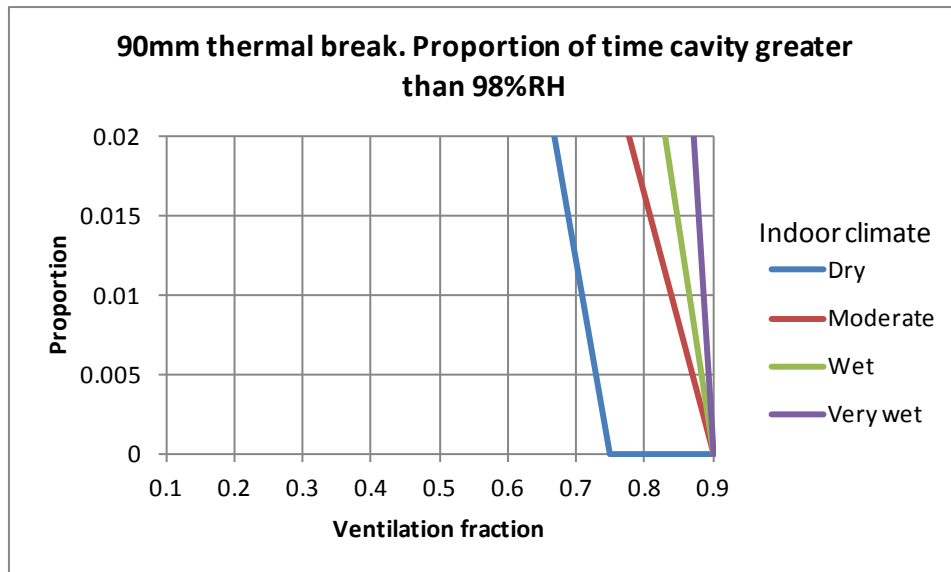


Figure 36: Design graph for a 90 mm thermal break (timber) and no board insulation. There is very little difference in performance between a timber and EPS thermal break.

The resulting design graphs are shown in Figure 37 and Figure 38. These graphs enable the designer to decide upon what proportion of time is acceptable for the cavity which is greater than 98%, then choose the insulation thickness and roof ventilation levels or modify the indoor climate to achieve that goal.

8.5 Achieving the required ventilation levels

Achieving a given ventilation level is not yet an exact science and there are no standard design methods to calculate what ventilation levels can be expected when placing a combination of vents in a combination of sites. BRANZ's WAVE programme will address some of those issues in the next year or two.

This work has shown that, for the ceiling type of interest (acoustic tiles and fibreglass insulation) under calm conditions, there is a ceiling air flow of around 5 m³/h, expressed per unit of area 0.2 m³/(m² h). We also note that for our specimen with no soffit level vents and with the ridge sealed we nevertheless get an outdoor-roof space flow level of around 15 m³/h. In other words, without making any attempt to ventilate the roof we still have a ventilation ratio of 15/20 = 0.75. With this in mind we can assume that any reasonable combination of soffit and ridge vents such as those found in overseas standards [15, 16] see Appendix, should guarantee a ventilation ratio higher, possibly much higher, than 0.75 putting us in a very favourable place on the design curves.

It is possible to explore this issue more deeply; for example a recent paper by Wang and Shen [17] uses computational fluid dynamics (CFD) to explore the effects of different vent size and positions on the resulting rate of ventilation. An approach using the known pressure coefficients [18] across the roof and knowledge of the flow characteristics of ventilators used is doable in principle.

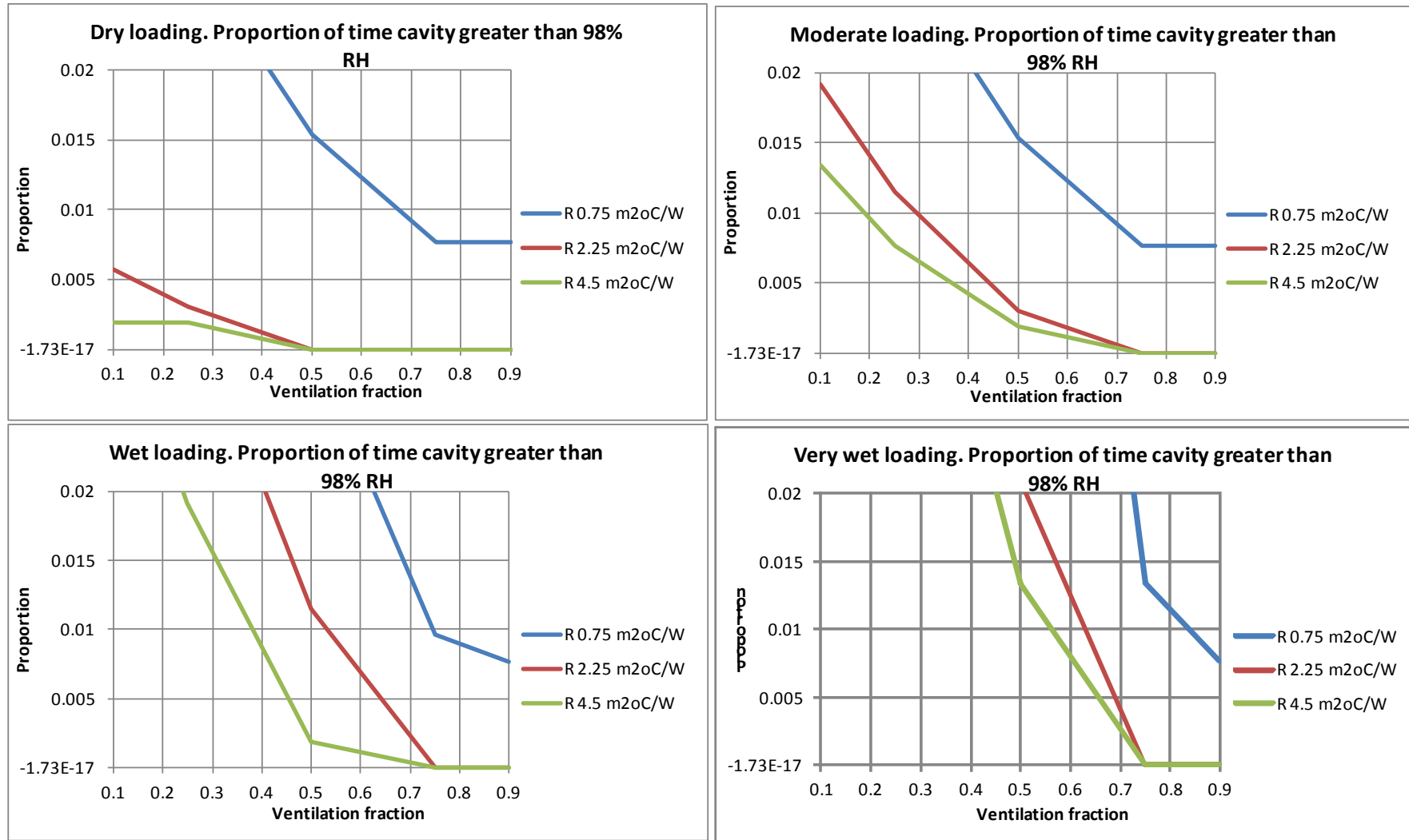


Figure 37: Design graphs by loading for specimens with rigid insulation systems above the main cavity.

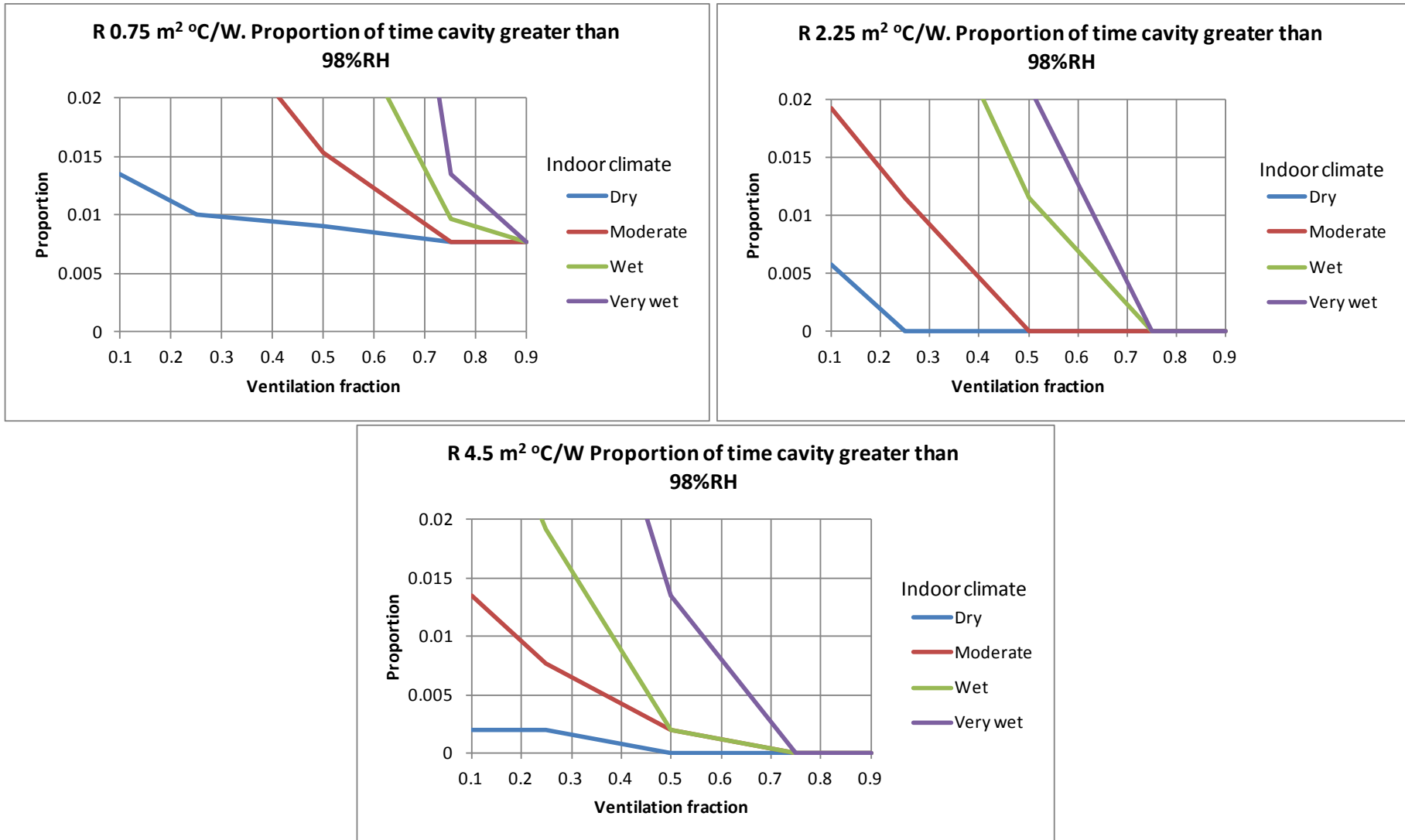


Figure 38: Design graphs by the R-value of the rigid insulation systems above the main cavity.

9. FURTHER WORK

We have only considered the climate of Dunedin in this work. Dunedin is in the coldest climate zone, i.e. climate zone 3, so designs here will be slightly conservative in climate zones 1 and 2.

Designs with no insulation on the ceiling, just EPS at the roof level, could also be considered. Ceiling insulation is often disturbed by people accessing and altering above ceiling services and can be a nuisance and become relatively ineffective.

10. DESIGN CONCLUSIONS

It is clear that roofs of the sort under study, viz roofs with large roof cavities, profiled metal roofs with underlay, metal framing, batt insulation on the ceiling and acoustic tile suspended ceilings, are vulnerable to episodes of condensation. We assume in this design section that a suspended ceiling is a requirement and therefore that it is not possible to change the ceiling system to easily improve its airtightness. Figure 36 shows that it is very difficult to design such a roof that avoids extensive periods of time above 98% relative humidity. On the other hand placing an insulation system above the main cavity increases the temperature of the metal purlins and the cavity air, and provides a system with good hygrothermal performance.

Design curves, Figure 37 and Figure 38, suggest the R-value of the insulation system above the main cavity should be at least $2.25 \text{ m}^2 \text{ }^\circ\text{C/W}$, that values higher than this are reaching the level of diminishing returns, and that ventilation fractions of 0.75 or better are also needed.

For the specimens examined in this work, the ventilation fraction was 0.97. This ventilation fraction was achieved without any conscious ventilation design (i.e. introducing vents) and indeed it was measured with the roof ridge sealed. Therefore by using any sensible choice of venting options, such as those found in overseas building codes, see Appendix, a higher ventilation fraction should be achieved.

The EPS system used as one of the specimen types in this study is relatively cheap, does not load the EPS structurally, and by appropriate choice of materials it should be possible to have it meet fire regulatory requirements.

11. GENERAL CONCLUSIONS

The hygrothermal performance of four different roof specimens has been examined experimentally and with models. Critical to the experimental success of the study was the accurate and non-linear calibration of relative humidity sensors in the difficult range of 95% to 100% RH. Good agreement between model and experimental temperatures has been obtained, and good agreement with relative humidities obtained also if the ventilation fraction is used as a fitting parameter.

It was found that the ventilation rates in these roofs will be in the range of 1 to 20 ach and that the roofs' performance were dominated by these ventilation-driven moisture fluxes over both diffusion from indoors and outdoors, and moisture transfers between the cavity air and hygroscopic materials in the roofs. This dominance was quantified with two dimensionless numbers, C_e and C_i . The ventilation fraction α , the proportion of ventilation coming from outdoors to total ventilation, is a key factor in determining the hygrothermal performance of these roofs.

Unexpectedly for the driving climates experienced there was often no condensation or frost under the metal roof when the roof was below the ambient dewpoint temperature. The data shows clearly that relative humidities and vapour pressures under the roof leave their expected trajectories as condensation conditions approach. This is due to hygroscopic absorption by the building underlay which prevents the relative humidity from rising to 100%. This is reflected in the very small value for the dimensionless number C_i for this small cavity above the underlay, implying that hygroscopic exchanges easily dominate over ventilative moisture fluxes in this cavity.

The timber specimen was found to absorb moisture hygroscopically during rain and release that moisture the next morning as the rising sun heats the roof up. The quantity released was found to be enough to trigger a condensation event.

The modelling was used to draw up graphs that enable the designer to choose the insulation thickness and roof ventilation levels or modify the indoor climate to limit the amount of condensation that may accumulate in these structures.

The EPS system used as one of the specimen types in this study does not load the EPS structurally and by appropriate choice of materials it should be possible to have it meet fire regulatory requirements.

This project did not attempt to examine any ceiling systems other than a suspended ceiling. Future work, under the WAVE project, will examine ceiling systems of different airtightness.

12. REFERENCES

1. EN ISO 14683. *Thermal bridges in building construction: linear thermal transmittance, Simplified methods and default values; 2000.*, 2000.
2. *Thermal bridges in building construction. Heat flows and surface temperatures. Detailed calculations, EN 10211, ISBN: 978 0 580 64346 0.*
3. Houses, N.A.o.S.-F., *N-10 Thermal break and cavity construction*, 2009.
4. Susanti, L., H. Homma, and H. Matsumoto, *A naturally ventilated cavity roof as potential benefits for improving thermal environment and cooling load of a factory building.* Energy and Buildings, 2010.
5. MA, F.-q., Y.-d. ZHOU, and L. GAO, *Analysis of Heat and Moisture Characteristics on the Building Roof of Steel Structure.* Science Technology and Engineering, 2008. **11**: p. 071.
6. Gorgolewski, M., *Developing a simplified method of calculating U-values in light steel framing.* Building and Environment, 2007. **42**(1): p. 230-236.
7. Zalewski, L., et al., *Experimental and numerical characterization of thermal bridges in prefabricated building walls.* Energy Conversion and Management, 2010. **51**(12): p. 2869-2877.
8. Standards, B., *BS 5250:2002 Incorporating Amendment No. 1. Code of practice for control of condensation in buildings*, 2002.
9. Burch, D., G. Tsongas, and G. Walton, *Mathematical analysis of practices to control moisture in the roof cavities of manufactured houses.* Nistir 5880, 1996.
10. Sanders, C., *Technical Summary of Partners in Innovation Project Improved Thermal and moisture Performance of Pitched Roofs.* Glasgow Caledonian University Report, 2005.
11. Nelson, P.E. and J.S.D. Ananian, *Compact Asphalt Shingle Roof Systems: Should They be Vented?* Journal of ASTM International, 2009. **6**(4).
12. *WUFI-2D*, A.d.h.a.m.t. program, Editor: Fraunhofer-Institut für Bauphysik.
13. Quaglia, M.J.C.L., *The Hygrothermal Performance of Building Underlays under Metal Roofs.* In preparation, 2013.
14. Cunningham, M.J., *Effective penetration depth and effective resistance in moisture transfer.* Building and Environment, 1992. **27**(3): p. 379-386.
15. *Code of Practice for control of condensation in buildings*, in *British Standard BS 5250:2002*.
16. *International Building Code 2012 (Second printing)*, 2012.
17. Wang, S. and Z. Shen, *Impacts of Ventilation Ratio and Vent Balance on Cooling Load and Air Flow of Naturally Ventilated Attics.* Energies, 2012. **5**(9): p. 3218-3232.
18. Kobayashi, T., et al., *Experimental Investigation and CFD Analysis of Cross-Ventilated Flow through Single Room Detached House Model.* Building and Environment, 2010. **45**(12): p. 2723-2734.

13. APPENDIX

13.1 Ventilation requirements in some overseas building codes

International Building Code (IBS)

This Code is international in the same sense that the World Series of Baseball is international, i.e. it was developed and is used in the USA and resulted from the amalgamation of three regional USA Codes.

Commercial buildings in the USA are usually required to ventilate according to Section 1503.5 and 1203.2 of the International Building Code, 2012 (Second Printing), which states:

1503.5 Roof ventilation

Intake and exhaust vents shall be provided in accordance with Section 1203.2 and the manufacturer's installation instructions.

1203.2 Attic spaces

Enclosed *attics* and enclosed rafter spaces formed where ceilings are applied directly to the underside of roof framing members shall have cross ventilation for each separate space, by ventilation openings protected against the entrance of rain and snow. Blocking and bridging shall be arranged so as not to interfere with the movement of air. An airspace of not less than one inch (25 mm) shall be provided between the insulation and the roof sheathing. The net free ventilating area shall not be less than 1/150th of the area of the space ventilated.

Exceptions:

1. The net free cross-ventilation area shall be permitted to be reduced to $1/300$ provided that not less than 50% and not more than 80% of the required ventilating area provided by ventilators located in the upper portion of the space to be ventilated at least three feet (914 mm) above eave or cornice vents with the balance of the required *ventilation* provided by eave or cornice vents.
2. The net free cross-ventilation area shall be permitted to be reduced to $1/300$ where a Class I or II vapour barrier is installed on the warm-in-winter side of the ceiling.

BS 5250:2002 "Code of Practice for control of condensation in buildings" Amendment 1

Where counterbatten venting is called for by this Standard the underlay should be at least 25 mm above the insulation at the centre of its droop.

A vapour barrier of at least 250 MNs/g is required in this Standard for flat roofs.

		Large voids (pitched roofs). Attic ventilation					Small voids (skillion roofs) PROVIDE A VAPOUR BARRIER			
		Low vapour resistance underlay ($\leq 0.25\text{MNs/g}$)		High vapour resistance underlay ($> 0.25\text{MNs/g}$)			Low vapour resistance underlay ($\leq 0.25\text{MNs/g}$)		High vapour resistance underlay ($> 0.25\text{MNs/g}$)	
		Ceiling well sealed	Normal ceiling	Slope $<15^\circ$	Slope $>15^\circ$	Slope $>35^\circ$	Well sealed		Normal ceiling	
Cladding air-loose	Cladding not air-loose. Requires counter batten ventilation									
Dwelling	Eaves	3	7	25	10	10	No requirement	25	25	25
	Ridge		or 5			& 5		& 5	& 5	& 5
Larger than dwelling	Eaves	5	10							
	Ridge	& 5	& 5							

Table 8: Ventilation requirements (in units of 1000 mm²/m roof width or equivalently height in mm of a continuous vent opening) for roofs under BS 5250:2002, Amendment 1 [15]

The high vapour resistance underlay option is not available in New Zealand. Where it is used in the UK there is the requirement that: pitched roofs have very good attic ventilation; or skillion roofs have good above-the-underlay ventilation or that the ceiling is very well sealed.

The Standard does allow for a well-sealed ceiling but it does acknowledge that that is very difficult to achieve.

“8.4.1.2 Air tightness of sloping and horizontal ceilings ... however a totally airtight ceiling is extremely difficult to achieve in practice. A well-sealed ceiling requires the following:

- a) The design avoids constructional gaps, especially at the wall/ceiling junction with dry lining construction and holes in the ceiling.
- b) No access door or hatch should be located in rooms where large amounts of moisture are produced, including kitchens or bathrooms.
- c) The air leakage rate through an access hatch, including its frame, when tested to BS EN 13141-1:2004 **4.3** is less than 1 m³/h at a pressure difference of 2 Pa. It can be assumed that “pushup” wooden hatch covers in a frame, constructed in-situ, with continuous compressible seals, will meet this criterion provided the weight of the door is at least 5.5 kg. Hatch covers should either be heavy enough to compress a seal or be clamped, with a closed cell compressible seal, or “O-ring” between it and the frame. Drop-down hatch covers are more difficult to seal; it is recommended that proprietary units with a supplied hatch cover in a frame are used. Manufacturers can provide third-party evidence that the leakage criterion is met.
- d) Penetrations, such as those for services and rooflights, are permanently sealed with suitable proprietary products.
- e) The ceiling is sealed to the external walls to limit any leakage through cracks.
- f) Recessed light fittings should either comply with BS EN 60529 and be rated IP60 to IP65 (depending on room use) or incorporate an appropriate sealed hood or box which meets the following test criteria. The total leakage through all downlighters should not exceed 0.06 m³/h·m² of ceiling at 2 Pa. The leakage of individual downlighters can be tested using the method specified in **4.3** of BS EN 13141-1:2004.
- g) The head of any cavity in any wall or partition should be sealed to prevent transfer of warm moist air into the loft.”